

Review Article

Open Access



Recent progress in soft electronics and robotics based on magnetic nanomaterials

Xiang Lin¹, Mengdi Han^{2*}

¹School of Biomedical Engineering, Shenzhen Campus of Sun Yat-sen University, Shenzhen 518000, Guangdong, China.

²Department of Biomedical Engineering, College of Future Technology, Peking University, Beijing 100871, China.

*Correspondence to: Prof. Mengdi Han, Department of Biomedical Engineering, College of Future Technology, No. 5 Yiheyuan Road, Haidian District, Peking University, Beijing 100871, China. E-mail: hmd@pku.edu.cn

How to cite this article: Lin X, Han M. Recent progress in soft electronics and robotics based on magnetic nanomaterials. *Soft Sci* 2023;3:14. <https://dx.doi.org/10.20517/ss.2023.05>

Received: 1 Feb 2023 **First Decision:** 6 Mar 2023 **Revised:** 26 Mar 2023 **Accepted:** 15 Apr 2023 **Published:** 9 May 2023

Academic Editors: Yihui Zhang, Young Min Song **Copy Editor:** Dong-Li Li **Production Editor:** Dong-Li Li

Abstract

Recent advancements in soft electronics and robotics have expanded the possibilities beyond the capabilities of traditional rigid devices, indicating promise for a range of applications in electronic skins, wireless biomedical devices, and others. Magnetic materials exploited in these soft systems can further broaden the modalities in sensing and actuation. These magnetic materials, when constructed in the forms of nanoparticles, nanomembranes, or other types of nanostructures, exhibit some unique characteristics, such as the magnetoresistance effect and size-dependent coercivity. Soft electronics and robotics employing such magnetic nanomaterials offer a variety of functions, including the detection of the intensity and direction of magnetic fields, measurement of various types of mechanical deformations, manipulation and transport at small scales, and multimodal complex locomotion in a controllable fashion. Despite recent advancements in soft electronics and robotics, challenges remain in developing advanced materials and manufacturing schemes to improve performance metrics and facilitate integration with other devices. This review article aims to summarize the progress made in soft electronics and robotics based on magnetic nanomaterials, with an emphasis on introducing material and device performance. The discussions focus on soft electronics and robotics based on magnetic nanomembranes/nanostructures and magnetic composites. As a concluding remark, this article summarizes the current status of the field and discusses opportunities that underpin future progress.

Keywords: Soft electronic, soft robotics, magnetic nanomaterials



© The Author(s) 2023. **Open Access** This article is licensed under a Creative Commons Attribution 4.0 International License (<https://creativecommons.org/licenses/by/4.0/>), which permits unrestricted use, sharing, adaptation, distribution and reproduction in any medium or format, for any purpose, even commercially, as long as you give appropriate credit to the original author(s) and the source, provide a link to the Creative Commons license, and indicate if changes were made.



INTRODUCTION

In recent years, advances in materials and manufacturing approaches have inspired a diverse set of soft electronics and robotics with performances comparable to conventional rigid devices^[1-7]. The flexibility and stretchability of these soft systems offer tremendous potential applications in many aspects, including but not limited to electronics/optoelectronics, microelectromechanical systems (MEMS), energy harvesting and storage devices, electronic switches, healthcare monitoring systems, and other biomedical tools^[8-17]. Compared to rigid devices, soft electronics with mechanical similarity to biological tissues ensure intimate contact at the interface, enabling high-quality data acquisition with reduced noise and artifacts^[18-20]. For soft robotic systems, including soft actuators, major advantages involve capabilities of adaption, continuous deformation, environmental responsiveness and less damage to delicate objects^[21-26]. The soft form factor of these systems also allows them to withstand bending, stretching, folding, and other means of mechanical deformations^[27-29], thus providing possibilities for further miniaturization/integration and expanding the application scenarios to electronic textiles, sensory skins, and minimally invasive surgeries^[30-38].

Among various types of functional materials exploited in soft electronics and robotics, magnetic materials are of interest due to their unique properties in sensing and actuation. Compared to conventional magnetic materials, magnetic nanomaterials demonstrate some unique advantages. Firstly, magnetic materials in the form of nanomembranes or nanostructures can produce magnetoresistance (MR) effects, thereby expanding the sensing ability of magnetic sensors^[39,40]. Secondly, magnetic materials at the nanoscale show size-dependent coercivity, offering great potential for programmable deformation and tunable torque. Thirdly, mixtures of magnetic particles/nanowires and polymer matrices exhibit low effective modulus and can be magnetized in a programmable format through advanced manufacturing approaches, creating a diverse set of soft structures with enhanced capabilities in sensing and actuation. Incorporating these magnetic nanomaterials into soft electronic systems allows for the detection of the intensity and/or direction of magnetic fields generated from the earth^[41] or human body^[42-44], providing opportunities for wearable navigation and fundamental studies of electrophysiology^[45-47]. In robotic applications, besides the advantages of remote controllability and transparency to biological tissues^[48-51], magnets in nanoscale or mixed in polymer matrix can possess programmed magnetization profiles to produce various complex deformations and abundant motion sequences^[52-55]. Further developments in magnetic nanomaterials can continue to promote the performances and broaden the functions of soft electronics and robotics.

A series of reviews, in a general sense, have covered topics ranging from nanomaterials-enabled electronics and robotics^[56,57] to mechanisms and materials of magnetic devices^[58-60]. While many review articles have provided valuable insights into the development of materials, structures and manufacturing approaches for soft electronics and robotics, few have focused specifically on soft electronics and robotics based on magnetic nanomaterials. Recent works have shown that magnetic nanomaterials have the potential to expand the functions or promote the performances of many electronic and robotic systems in areas such as biomedicine, sensing, and human-machine interaction. Therefore, this review article aims to discuss magnetic nanomaterials and their applications in soft electronics and robotics to provide an overview of the latest developments in this field. In [Figure 1](#) and [Table 1](#), we categorize magnetic nanomaterials into two groups: magnetic nanomembranes/nanostructures (i.e., materials with thicknesses in nanoscale or with nanoscale patterns) and magnetic composites (i.e., mixtures of polymer matrices and magnetic particles). Sections “Soft electronics based on magnetic nanomembranes/nanostructures” and “Soft electronics based on magnetic composites” introduce the progress of soft electronics based on magnetic nanostructures/nanomembranes and magnetic composite materials, respectively. Sections “Soft robotics based on magnetic nanomembranes/nanostructures” and “Soft robotics based on magnetic composites” continue to describe the applications of magnetic nanostructures/nanomembranes and magnetic composites, respectively, with a

Table 1. Representative magnetic nanomaterials

Type	Working principle	Representative materials	Manufacturing approaches	References
Nanomembranes/nanostructures	GMR effect	Co/Cu, NiFe/Cu	Molecular beam deposition, sputtering, electrodeposition, printing	[72,73,81]
	AMR effect	NiFe, NiCo	Sputtering, thermal evaporation	[87,91,95]
	TMR effect	CoFeB/MgO/CoFeB, Co/Al ₂ O ₃ /Alq ₃ /NiFe	Sputtering, transfer printing	[99,100,104]
Magnetic composites	Hard-magnetic	NdFeB particles, CrO ₂ particles	3D printing, molding, laser heating	[146,160,164]
	Soft-magnetic	Iron particles, NiFe particles	Soft lithography, magnetic field-assisted molding	[126,128,170]
	Superparamagnetic	Iron oxide nanoparticles	Thermal curing, laser/mechanical cutting	[149,150,165]

AMR: Anisotropic magnetoresistance; GMR: giant magnetoresistance; TMR: tunneling magnetoresistance.

focus on robotic systems. In the end, a concluding section summarizes the main advantages and applications of soft electronics and robotics based on magnetic nanomaterials, and presents some thoughts for the further development of this field.

SOFT ELECTRONICS BASED ON MAGNETIC NANOMEMBRANES/NANOSTRUCTURES

Electronic devices that can detect the intensity and direction of magnetic fields are important for applications spanning from motion tracking in consumer electronics to *in vitro* assays in biomedicine^[61,62]. Soft electronics with such capabilities provide additional possibilities, such as on-skin, tattoo-like navigation, and *in vivo* multimodal sensing. Superconducting quantum interference device (SQUID) and optical-pumping magnetometer (OPM) are important techniques for magnetic field sensing, but they require low temperatures, bulky wires, or optical fibers that are not compatible with soft electronics^[63-66]. In contrast, the MR effect relies on materials constructed in the format of nanomembranes or other nanostructures to detect magnetic fields. The ultrathin feature (thickness in the nanoscale) of these materials allows for their construction in a miniaturized and flexible format. In Sections “Soft electronics based on GMR effect”, “Soft electronics based on AMR effect”, and “Soft electronics based on TMR effect”, we discuss soft electronics based on giant magnetoresistance (GMR), anisotropic magnetoresistance (AMR), and tunneling magnetoresistance (TMR) effects, respectively.

Soft electronics based on GMR effect

The GMR effect primarily relies on multilayer nanostructures made up of alternating ultrathin ferromagnetic (FM) and non-magnetic (NM) conductive layers, each with a thickness of a few nanometers^[67-69]. Figure 2A shows the schematic illustration of a simplified GMR sensor, where one NM layer is sandwiched between two FM layers. In the absence of a magnetic field, the FM layers are in a random magnetization direction, and can be modeled as antiparallel configurations using a tri-layer structure [middle frame of Figure 2A]. In this case, both spin-up and spin-down electrons encounter strong scattering, thereby causing high resistance. When an external magnetic field is applied, the FM layers can be induced into parallel alignment, allowing spin-up electrons to pass through with little scattering, and strongly scattering spin-down electrons. The clear paths for spin-up electrons result in low electrical resistance of the GMR structure [right frame of Figure 2A]. Recent advancements in material science and electrical engineering yield a diverse set of GMR structures, including magnetic multilayer structures, spin valve trilayer structures, and magnetic granular structures^[70,71], with materials ranging from multilayers of Co/Cu to NiFe/Cu and others^[72,73]. Among the various GMR structures, the spin valve trilayer structures

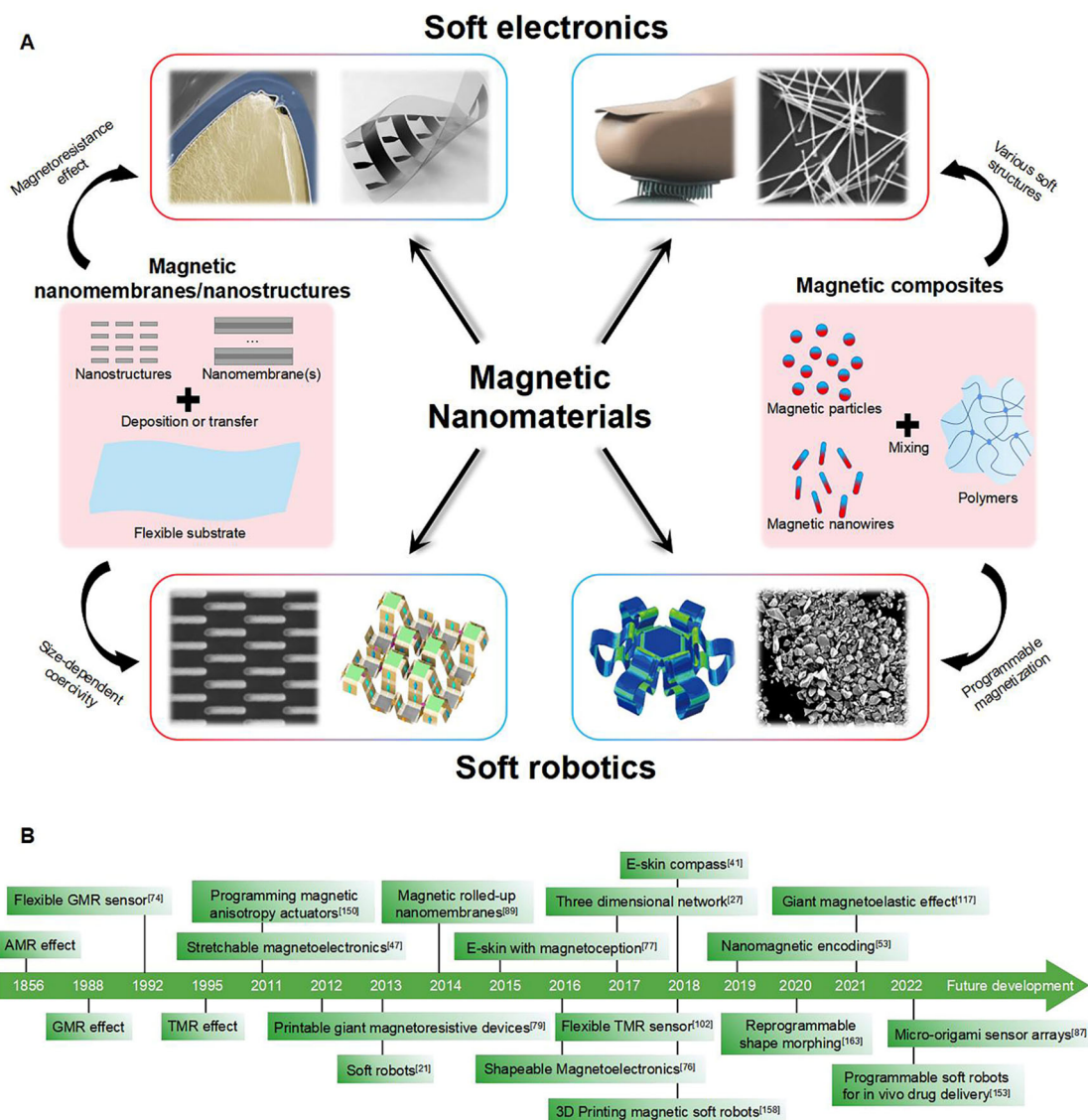


Figure 1. Overview of soft electronics and robotics based on magnetic nanomaterials. (A) Classification and representative examples; (B) Chronology of publications and intellectual properties (patents).

exhibit a linear response of resistance under a magnetic field, making them ideal basic components for magnetic sensors^[73].

Such magnetic sensors are based on nanomembranes of multiple materials configured in a multilayer format. The ultrathin feature provides immediate opportunities to construct soft magnetic sensors by depositing NM and FM layers on flexible polymer substrates. Another advantage of GMR sensors is that the materials deposited directly on polymer substrates can also exhibit sufficient sensitivities for many applications. For example, Parkin *et al.* demonstrate that multilayers of Co/Cu (thickness: 1 nm for one layer of Co, 0.9 nm for one layer of Cu) deposited onto Kapton films display large room-temperature magnetoresistance, with MR ratios of up to 65%, comparable to those found in similar structures prepared on silicon wafers^[74].

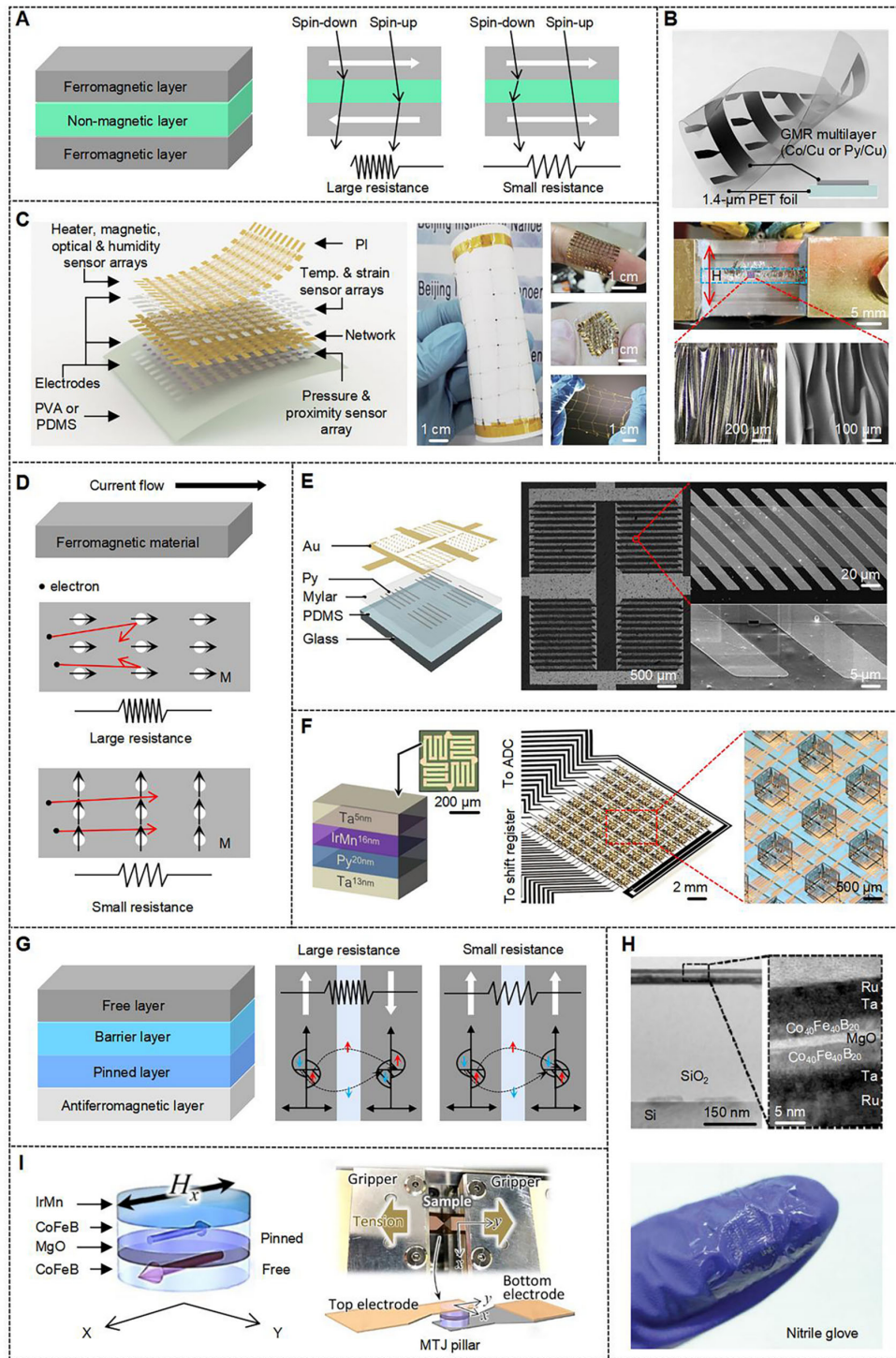


Figure 2. Soft electronics based on magnetic nanomembranes/nanostructures. (A) Schematic illustration of the structure and mechanism of a simplified trilayer GMR sensor; (B) An imperceptible magnetic sensor foil consisted of GMR sensors. Top frame: structure of the sensor. Middle frame: optical image of a sample (marked by the blue dashed rectangle) mounted to a stretching stage. Bottom frames: scanning electron microscopy (SEM) images of the sample under 50% compressive strain. The red arrow indicates the direction of the applied magnetic field. Reproduced with permission from Ref.^[77]. Copyright © 2015. Springer Nature; (C) An SCMN with eight functions. Left frame: schematic illustration (temp.: temperature). Right frames: optical images of the SCMN attached to a sheet of paper, integrated on a human finger and human skin, and stretched manually. Reproduced with permission from Ref.^[78]. Copyright © 2018. Springer Nature; (D) Schematic illustration of the structure and mechanism of an AMR sensor; (E) An e-skin compass. Left frame:

structure of the device. Right frames: optical micrography of the e-skin compass. Reproduced with permission from Ref.^[41]. Copyright © 2018. Springer Nature; (F) An active matrix consisting of micro-origami sensor arrays. Left frame: structure of the device. Inset of the left frame shows the micrograph of the AMR sensors. Right frame: optical image of an integrated micro-origami magnetic sensor device with 8×8 pixels. Right frame: magnified view of several pixels. Reproduced with permission from Ref.^[87]. Copyright © 2022. Springer Nature; (G) Schematic illustration of the structure and mechanism of a TMR sensor; (H) A flexible TMR sensor. Top frames: transmission electron microscopy (TEM) images of the MTJ structure. Bottom frame: optical image of MTJs transferred onto nitrile glove. Reproduced with permission from Ref.^[104]. Copyright © 2016. John Wiley and Sons; (I) A film-type strain gauge with the exchange-biased MTJ. Left frame: schematic illustration of the device. Top right frame: optical image of the motor-driven tensile machine for the sample. Bottom right frame: illustration of structure. Reproduced with permission from Ref.^[107]. Copyright © 2022. AIP Publishing. AFM: Antiferromagnetic; AMR: anisotropic magnetoresistance; GMR: giant magnetoresistance; MTJs: magnetic tunneling junctions; PET: polyethylene terephthalate; SCMN: stretchable and conformable matrix network; TMR: tunneling magnetoresistance.

One important direction of soft GMR sensors focuses on investigating the influence of different flexible substrates on the performance of the GMR device, in order to develop magnetic sensors with desired sensitivity, flexibility and mechanical endurance for applications in biomedicine or other bio-integrated systems^[75,76]. Figure 2B introduces electronic skins (e-skins) integrated with GMR sensors. Such e-skins allow wearers to perceive the presence of static or dynamic magnetic field, thereby expanding the sensing capability of the human body. Here, the highly sensitive GMR sensor elements are on an ultrathin (thickness: $1.4 \mu\text{m}$) polyethylene terephthalate (PET) foil with mechanical properties of light weight and high strength. The GMR sensors exhibit high sensitivities of up to $0.25\% \text{ Oe}^{-1}$, identical to their counterparts on rigid Si/SiO₂ wafer substrates. The e-skins are thin enough to provide an imperceptible feature during wearing and can withstand cyclic tensile strains (270%, 1000 cycles) without fatigue^[77].

The incorporation of photolithographic techniques into these magnetoelectronic nanomembranes on ultrathin plastic foils enables the fabrication of devices with accurate patterns over large areas and in a multiplexed array format. These resulting sensor arrays exhibit flexibility, stretchability, and mechanical robustness and can integrate with other soft electronics to form a multifunctional system. Figure 2C shows a skin-inspired, highly stretchable and conformable matrix network (SCMN) that combines multiple functions, including but not limited to the sensing capabilities of temperature, in-plane strain, humidity, light intensity, magnetic field, pressure, and proximity^[78]. The multilayer design [left frame of Figure 2C] separates six different types of sensor units in different layers to avoid complicated wiring. The magnetic field sensors exploit multilayers of Co/Cu as the GMR elements (MR ratios: 50%), and locate in the middle of the multilayer stacks. The combination of magnetic field sensors with other devices allows for simultaneous measurements of various signals induced by the external environment, providing immediate applications in navigation, touchless control, and human-machine interface.

Other examples of soft electronics based on GMR nanomembranes include printable GMR sensors for low-cost large-area production and easy integration with wearable devices and textiles^[79,80], highly integrated magneto-sensitive electronic membranes for extensive applications in the field of interactive electronics^[81,82], GMR 3D angular encoders with high angular accuracy in all directions^[83], and many more^[84-86].

Soft electronics based on AMR effect

Compared with GMR nanomembranes, whose resistance only depends on the intensity of the magnetic field, the resistance change of AMR sensors depends on both the intensity and the direction of the magnetic field. The AMR effect is an important physical phenomenon in spintronics, where the angle between the current flow and magnetization direction determines the resistance of the ferromagnetic material [Figure 2D]. Compared with GMR sensors, AMR sensors usually have a smaller resistance change under a magnetic field. However, the capability to distinguish the direction of magnetic field underpins unique

applications of AMR sensors.

Figure 2E shows an example of using nanomembranes of $\text{Fe}_{81}\text{Ni}_{19}$ alloy (thickness: 50 nm) as AMR sensors for an on-skin compass^[41]. The layout of the compass exploits a Wheatstone bridge configuration to connect four AMR sensors [right frame of Figure 2E]. The compass uses silicone elastomer as the substrate and gold thin film (thickness: 100 nm) as the contact and conditioning layer. These thin film materials render a highly compliant compass that can form intimate, conformal contact with the skin. It shows sufficient sensitivity (0.54 mT^{-1} for a single sensor) to geomagnetic fields (40-60 μT), and functions properly under cyclic bending with a radius of curvature of 150 μm . The AMR-based on-skin device can fully replicate the functionality of a compass, thereby allowing people to orientate themselves with respect to the Earth's magnetic field for navigation purposes.

Most of the AMR sensors can only perceive field components in one or two dimensions, due primarily to the planar configurations of the devices. To expand the sensing capability to a third dimension (i.e., vertical direction), researchers exploit a self-folding process to construct high-density active matrix of magnetic sensors with three-dimensional (3D) geometries [Figure 2F]^[87]. Specifically, each sensing pixel consists of three AMR sensors folded in three orthogonal orientations to enable 3D magnetic vector field sensing. The AMR sensors are based on nanomembranes of NiFe alloy (thickness: 20 nm), and can be used for spatiotemporal mapping of 3D magnetic fields with a spatial resolution of 1.1 mm. In addition, the 3D magnetic sensor is capable of detecting the amplitude and direction of external mechanical stimuli by adding a flexible composite skin layer and embedded magnetic hairs.

As an important application in biomedicine, AMR sensors with a navigation function can integrate with various medical tools, such as biopsy needles, endoscopes and catheters, to allow physicians to track the positions and movements of medical tools inside human bodies without the use of harmful radiation or contrast agents^[88]. For example, a self-assembled catheter integrated with rolled-up flexible AMR sensors offers basic navigation functionalities with a resolution of 0.1 mm, similar to those of electromagnetic tracking^[89]. The strategy of deploying AMR sensors on medical tools constitutes a novel paradigm for the manufacturing of biomedical tools and has the potential to expand the boundary of minimally invasive surgery.

Other examples of soft electronics based on AMR nanomembranes include stable magnetic sensors with sensitivities comparable to GMR sensors on flexible substrates^[90], printable sensors with high performance and compliance^[91], magnetic angle sensors for angular position measurement in harsh environments^[92], and others^[93-95].

Soft electronics based on TMR effect

AMR and GMR sensors have great potential for use in soft electronics, yet the MR ratios are typically less than 5% for the former and around 50% for the latter^[96]. Such low MR ratios limit the sensitivity of AMR and GMR sensors and hinder their applications in detecting weak magnetic fields presented in biology^[97-99]. Meanwhile, the MR ratio can exceed 200% in magnetic tunneling junctions (MTJs)^[100] that exist in the TMR effect. Figure 2G depicts the structural schematic of an MTJ, composed of a free layer (FL), a barrier layer (an extremely thin insulator), a pinned layer (PL) and an antiferromagnetic (AFM) layer [left frame of Figure 2G], each with a thickness of a few nanometers. The AFM layer fixes the magnetization direction of the PL, while the magnetization direction of the FL can rotate under an external magnetic field. Thus, the MTJ structure can be considered as a sandwich heterojunction consisting of an insulating layer between two FM sheets. The two FM layers are in antiparallel configurations without any external interference [middle

frame of Figure 2G]. In this case, the electrons in the minority-spin sub-band of one FM layer tunnel into the majority-spin sub-band of the other layer, and those in the majority-spin sub-band enter the opposite, resulting in small tunneling current and high resistance. In another case where the two FM layers are in the same magnetization direction, the electrons would pass into the consistent sub-band from one layer to the other, thereby leading to large tunneling current and low resistance [right frame of Figure 2G]. Since there is almost no interlayer coupling between the two FM layers, a small external magnetic field can change the magnetization direction of one layer and induce considerable resistance variation. Such processes render the high magnetic sensitivity of TMR sensors.

However, the fabrication of high-performance TMR materials usually requires an annealing process at elevated temperatures ($\geq 300^\circ\text{C}$) and high vacuum conditions^[101], which impedes the formation of TMR sensors on flexible polymer. The transfer printing process, which involves retrieving material from a carrying substrate and delivering it onto other flexible or stretchable substrates, can solve the problem to some extent^[102,103]. Figure 2H shows an example of flexible TMR sensors^[104]. Here, a conventional deposition process is used to form nanomembranes of CoFeB/MgO/CoFeB (thickness: 6/2/4 nm) on a thermally oxidized silicon substrate. By etching away the underlying silicon, the nanomembranes can be released and transferred onto various flexible substrates, including aluminum foil, silicone elastomer, nitrile glove, and others [bottom frame of Figure 2H]. In this particular case, the transfer process enhances the MR ratios to more than 200% (~ 1.38 times higher than the TMR prior to transfer), primarily due to the strain-induced change on quantum tunneling, which enables the development of flexible TMR sensors.

Although the transfer printing method enables the fabrication of relatively high-quality flexible MTJs, it complicates the manufacturing process. An alternative approach is to deposit TMR materials directly on flexible substrates with high thermal tolerance^[105,106]. Figure 2I demonstrates a highly sensitive thin-film strain gauge based on an MTJ formed on a thin flexible polyimide substrate (thickness: 50 μm)^[107]. Under an external magnetic field (intensity: 2 mT), the flexible MTJ with a pseudo-spin valve (SV) structure shows a much larger gauge factor (~ 1000) compared with conventional metal-foil strain gauges (gauge factor: ~ 2). Using strain-sensitive free layers and adding strain-insensitive exchange-biased pinned layers allow the MTJ to obtain stable performance without external magnets, thereby making it more suitable for practical applications.

Although transfer printing and direct deposition on high-temperature resistant materials provide effective means to fabricate soft TMR sensors, the fragile and strain-sensitive natures of the inorganic nanomembranes pose challenges in achieving stable electrical and mechanical performances. As a result, most TMR sensors still possess rigid form factors, targeting applications in areas ranging from robotic industrial control to consumer electronics and *in vitro* biosensing^[108-111].

SOFT ELECTRONICS BASED ON MAGNETIC COMPOSITES

Soft electronics based on magnetic nanomembranes/nanostructures have shown great potential in applications of multimodal e-skins, wearable navigation devices, and flexible mechanical sensors^[41,112,113]. Such systems mainly rely on structural designs (e.g., ultrathin layers, serpentine and/or other patterns) to achieve flexibility and stretchability. The materials themselves, especially those sensing elements (i.e., GMR, AMR and TMR materials), exhibit high modulus and are not intrinsically stretchable. These properties impede the conformal integration of magnetic sensors with soft biological tissues, and limit the degree of freedom of deformations. Unlike nanomembranes, which only have small dimensions in one direction (thickness), magnetic micro/nanoparticles and nanowires (NWs) possess small features in all directions and, therefore, can be well dispersed in other mediums to form magnetic composites. Adjusting the

material, weight ratio, and magnetization direction of the magnetic micro/nanoparticles serves as an effective approach to adjusting the tunable elastic and magnetic properties of the composites^[114,115].

Figure 3A illustrates a soft electronic system based on magnetic composites. The system consists of magnetic microparticles (neodymium iron boron (NdFeB), average particle radius: $\sim 5.00 \mu\text{m}$; remanence: 92.3 emu g^{-1} ; coercive magnetic field: 6375 Oe) and a porous silicone rubber matrix. The embedded ferromagnetic particles enable the system to convert mechanical deformations into electricity using coils. Compared with systems that mix the iron micro/nanoparticles with silicone rubber, the example shown in **Figure 3A** can generate electric signals in the absence of external magnetic fields, which simplifies the device configuration^[116,117].

In the process of heating the mixture of uncured silicone rubber and micro/nanomagnets, an option is to introduce air bubbles to form porous composites. Such porous structures not only reduce the modulus, but also provide tiny spaces for the micro/nanomagnets to reorientate and move during impulse magnetization, eventually forming a chain-like arrangement of the micromagnets associated with the giant magnetoelastic effect. Compared with the traditional magnetoelastic effect arising from magnetic domain rearrangement and stress-induced magnetic anisotropy under external magnetic field, this giant magnetoelastic effect is attributed to the change of micro-magnetic chain structure under mechanical deformation. As shown in the right frame of **Figure 3A**, compression changes the chain structure of the magnet, causing a decrease in surface magnetic flux density. The soft system can withstand a tensile strain of up to 190%, and demonstrates much lower modulus (at the level of 100 kPa), compared with conventional magnetic alloy (modulus at the level of 10 GPa)^[118]. Such features enhance the biomechanical-to-magnetic energy conversion and open many potential applications in soft electronics, including wearable/implantable energy harvesters, and stretchable biomedical sensors for continuous monitoring of human pulse waves and heart rhythms^[119].

Another advantage of magnetic composites is that the direction of magnetization can be programmed in a heterogeneous manner, as the composite materials are soft enough to be folded, wrapped, or otherwise deformed into 3D geometries during magnetization^[120,121]. In particular, magnetizing a flexible magnetic film with a sinusoidal pattern enables high spatial resolution and the capability to decouple different mechanical stimuli [**Figure 3B**]^[122]. The soft tactile sensor involves a soft magnetic composite (modulus: $\sim 2 \text{ MPa}$; thickness: 0.5 mm) formed by mixing polydimethylsiloxane (PDMS) and NdFeB magnetic powders with a weight ratio of 1:3, a silicone elastomer layer (Ecoflex 00-50, modulus: $\sim 83 \text{ kPa}$), and a commercial Hall sensor [left frame of **Figure 3B**]. The soft magnetic composite deforms under external force and causes a change in magnetic flux density, which can be detected by the Hall sensor embedded in the silicone elastomer [right frame of **Figure 3B**]. Here, the sinusoidal pattern (obtained by wrapping the soft magnetic composite on a cylinder during magnetization) is crucial for decoupling and super-resolution. On the one hand, the magnetic field distribution caused by the sinusoidal pattern is decoupled into two mutually orthogonal planes: the magnetic strength B and the magnetic ratio R_B . The B plane determines the normal force related to the magnetic field rotation angle (or displacement along the z -axis), while the R_B plane measures the shear force related to the translational movement of the magnetic field (displacement d along the x -axis). The capability to decouple various mechanical stimuli overcomes the inherent problem of the strong cross-coupling effects in conventional magnetic tactile sensors^[123-125]. On the other hand, extending the sinusoidal patterns to the form of sensor arrays allows for tactile sensing with super-resolution and across large areas. Combined with deep learning algorithm, the sensors can achieve a 60-fold improvement in localization (from 6 to 0.1 mm).

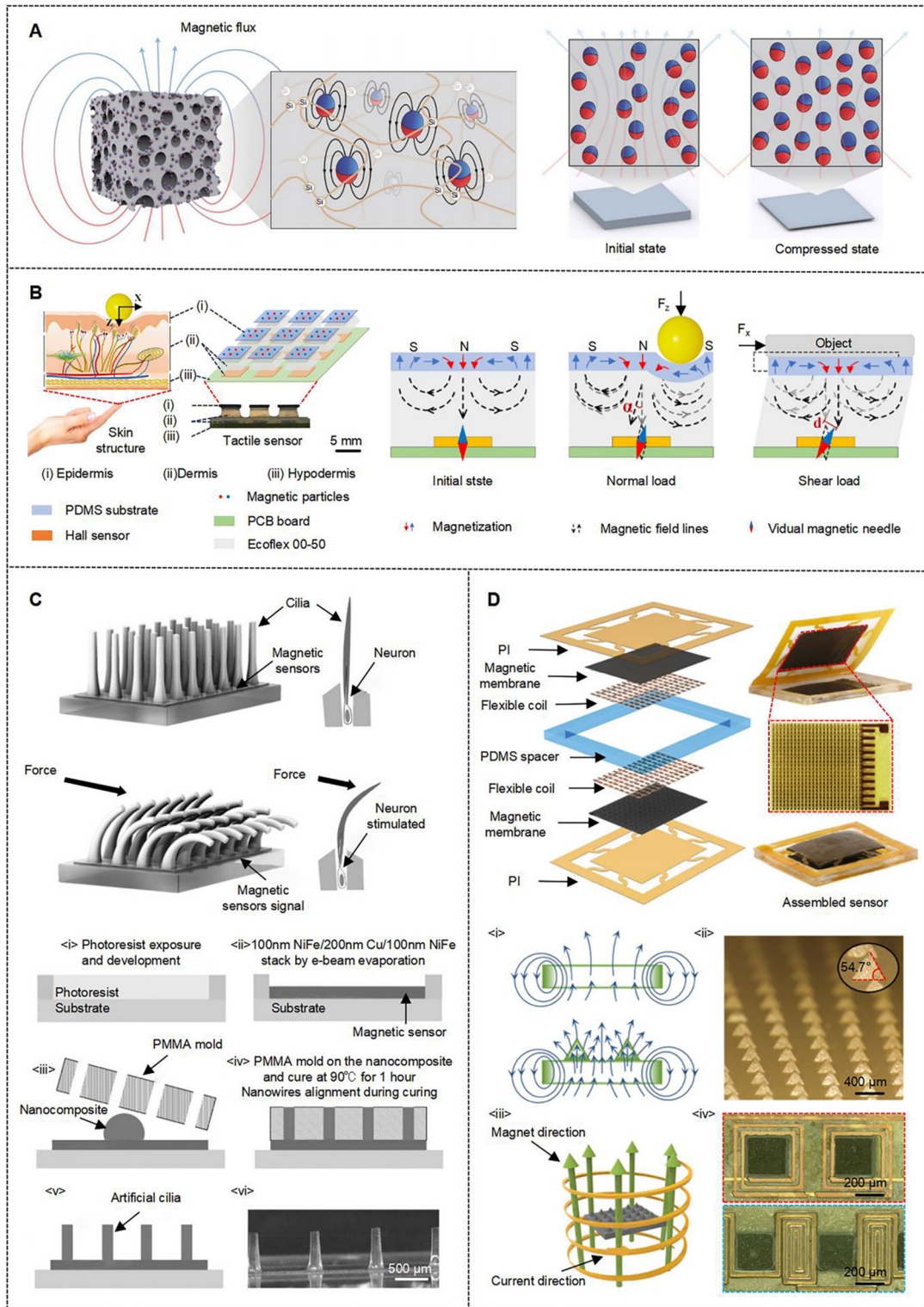


Figure 3. Soft electronics based on magnetic composites. (A) Giant magnetoelastic effect in a soft system. Left frame: sketch of the porous soft system and its internal structure. Right frame: illustration of the magnetic flux density of the soft system in the initial and compressed states. Spheres in red and blue colors represent micromagnets. Reproduced with permission from Ref. [118]. Copyright © 2021. Springer Nature; (B) Soft magnetic skin with force self-decoupled. Left frame: illustration of the human skin structure and the soft tactile sensor. Right frames: working principle of the tactile sensor. Reproduced with permission from Ref. [122]. Copyright © 2021. The

American Association for the Advancement of Science; (C) Nanocomposite cilia tactile sensor, which mimics the neuron in natural cilia. Top frames: schematic illustration of the sensor. Bottom frames: fabrication process of the tactile sensor. <i><ii> Deposition and pattern of permalloy/Cu/permalloy by e-beam evaporation and photolithography; <iii>-<v> Fabrication of the cilia using a PMMA mold. <vi> Optical images of the cilia. Reproduced with permission from Ref.^[128]. Copyright © 2015. John Wiley and Sons; (D) A magnetically levitated flexible vibration sensor with surface micropylramid arrays. Top frames: layer-by-layer structure and images of the assembled sensor. Bottom frames: <i> Schematics of the magnetic field distribution for membranes with and without microstructures. <ii> Image of the micropylramid arrays on a magnetic membrane. <iii> Illustration of the magnetization mechanism. <iv> Images of two types of coils surrounding the pyramid (red dashed rectangle) and between the pyramid (blue dashed rectangle). Reproduced with permission from Ref.^[129]. Copyright © 2022. American Chemical Society. GMI: Giant magneto-impedance; NdFeB: neodymium iron boron; PDMS: polydimethylsiloxane.

The above examples show the advantages of high elasticity and adjustable magnetization in using magnetic composites as planar, thin-film sensors. A remarkable feature of composites is that they can form various microstructures (e.g., cilia, pyramid) in pre-cured conditions by injection molding or other means^[126,127]. **Figure 3C** illustrates a magnetic tactile sensor based on highly elastic and permanent magnetic nanocomposite, constructed in the format of artificial cilia. The unique structure allows for measurements of a variety of mechanical stimuli, including normal pressure, shear force, surface texture, and flow. Similar to the mechanism in the neuron of natural cilia, the artificial magnetic cilia in the tactile sensor bend in the presence of external forces, causing changes in the magnetic field, which can be detected by a magnetic field sensor underneath the tactile sensor [upper frame of **Figure 3C**]^[128]. To form such devices, the nanocomposite is applied to the surface of a multilayer giant magneto-impedance (GMI) sensor (a 200 nm thick Cu layer sandwiched by two 100 nm thick Ni₈₀Fe₂₀ layers) with high sensitivity and solidified into cilia structures using a mold [lower frame of **Figure 3C**]. The nanocomposite mixes iron NWs (length: 6 μm, diameter: 35 nm) and PDMS to enable desired magnetic properties for sensing. The high elasticity and formability of the nanocomposite facilitate the adjustment of the dimensions of cilia, thereby offering means to achieve tunable resolution and sensitivity for various applications.

Changing the geometries of the molds provides a straightforward way to adjust the shapes of the microstructures. It has been proved that micropylramid structures can locally enhance the magnetism because they offer a magnetically permeable path to yield a more concentrated magnetic flux at the tip of each pyramid [**Figure 3D** <i>], with an increment of more than 35%. Magnetic membranes with such pyramid structures can be obtained by molding composites of microparticles (i.e., Nd₂Fe₁₄B) and PDMS, followed by magnetization along the thickness direction [**Figure 3D** <iii>]. The structured membrane contains an array of 24×24 micropylramids (interval distance: 440 μm), each with a length of 360 μm and a height of 254 μm [**Figure 3D** <ii>]. The upper frame of **Figure 3D** shows a levitated flexible vibration sensor based on two structured magnetic membranes, one of which is levitated by magnetic force. The levitated membrane vibrates under external disturbances, such as human motions and speaking. The vibration of the magnetic membrane changes the magnetic flux in the flexible electromagnetic coil arrays [**Figure 3D** <iv>], thereby inducing electromotive force voltage based on Lenz's law^[129].

In summary, magnetic composites have found wide applications in soft electronics due to their high elasticity and tunable structural geometry. The comparable elastic modulus of these sensors to that of human skin and tissues enables them to conformally adhere to irregular surfaces. Additionally, the tunable structural geometry of these sensors can improve their sensing performances and broaden their sensing modalities. Other examples in this area include highly efficient flexible and shapeable spin caloritronic devices^[130], thermo-responsive self-healing colloidal gels with potentially unusual magnetic and rheological responses^[131], and techniques for magnetic orientation control^[132].

SOFT ROBOTICS BASED ON MAGNETIC NANOMEMBRANES/NANOSTRUCTURES

Another significant application of magnetic nanomaterials is in the field of robotics. Magnetic actuation offers advantages over other actuation strategies such as light, thermal, and electric, including remote and wireless operation, which eliminates the need for optical fibers and electrical wires. Additionally, static and low-frequency magnetic fields do not attenuate through natural tissue and organs, making them suitable for use in biomedicine.

Magnetic nanomembranes in soft magnetic materials, such as iron, can be deposited and patterned using conventional microelectronic processes. Robots based on these materials, therefore, can have overall dimensions down to microscale, with promising applications in minimally invasive surgery and micromanipulation. **Figure 4A** shows an untethered magnetic gripper for single-cell manipulation^[133]. The gripper involves a bilayer of silicon monoxide and silicon dioxide (thickness: 30 nm in total) with internal stress mismatch to bend planar pattern into 3D geometries, a thin iron layer (thickness: 100 nm) for remote control under a magnetic field, and a thermally responsive layer made of wax for on-demand activation [middle frame of **Figure 4A**]. The gripper can be controlled remotely to navigate through narrow conduits and to fix tissue sections *ex vivo*. Compared with previously demonstrated grippers^[134-136], the gripper demonstrated in this example has a tip-to-tip size of 70 μm when open and 15 μm after folding. The dimension is comparable to the size of human arterioles (diameter: 50-300 μm), making the gripper suitable for future *in vivo* applications of cell capture or excision at the single-cell level.

Magnetostrictive materials can deform under the action of external magnetic fields and, therefore, represent promising candidates for constructing magnetic-controlled robots^[137,138]. Typical magnetostrictive materials involve Fe-Co-Ni-rich alloys, Terfenol-D, and Galfenol^[139-141]. These materials are also compatible with conventional microelectronic processes and can be deposited through magnetron sputtering coating. The example shown in **Figure 4B** proposes a method of directly depositing a magnetostrictive nanomembrane ($\text{Fe}_{50}\text{Co}_{50}$ alloy; thickness: 100 nm) on a flexible microfiber of spider silk thread (diameter: $9 \pm 5 \mu\text{m}$) in a scalable fashion. The resulting magnetostrictive fiber retains excellent properties in mechanical robustness, electrical conductivity, as well as magneto-mechanical coupling^[142]. For example, the fiber can maintain the original mechanical characteristics of spider silk to prevent irreversible plasticization, and exhibits capabilities in lifting loads up to 0.12 mN (maximal stress: $\sim 10 \text{ MPa}$) under a magnetic field of $\sim 0.1 \text{ T}$. These features allow the magnetic silk threads to serve as a basic component in soft robotics.

A noteworthy point of nanoscale magnetic materials is that their coercivities and remanences show dependence on their sizes^[143,144]. As shown in the coercivity curve in **Figure 4C**, the particles in cobalt have almost no remanence and coercivity at sizes smaller than 100 nm (regarded as superparamagnetic). When the size of cobalt is larger than the critical size (100 nm) but remains within hundreds of nanometers, the particles show single-domain characteristics, including high remanence and the positive correlation between coercivity and size. At scales larger than 500 nm, magnetic particles in cobalt exhibit multidomain features, where the coercivity reduces with the magnet size. Based on the effect that the coercivities of nanomagnets change with their sizes, researchers have developed a magnetic programming strategy that can encode multiple deformation instructions into magnetic robots^[53]. The four-panel robot in the left frame of **Figure 4C** is programmed by arranging panels with nanomagnets in different sizes (panel I: 520 nm \times 60 nm, illustrated with red color; panel II: 398 nm \times 80 nm, illustrated with blue color). Due to the positive correlation between coercivity and size, the robot can be coded through a series of magnetized fields in different intensities. For example, a magnetic field larger than 140 mT in one direction magnetizes both panel I and panel II. A subsequent magnetic field between 90 and 140 mT in the opposite direction reverses the magnetization of panel II. The intensity of the subsequent magnetic field ($< 140 \text{ mT}$) is not sufficient to

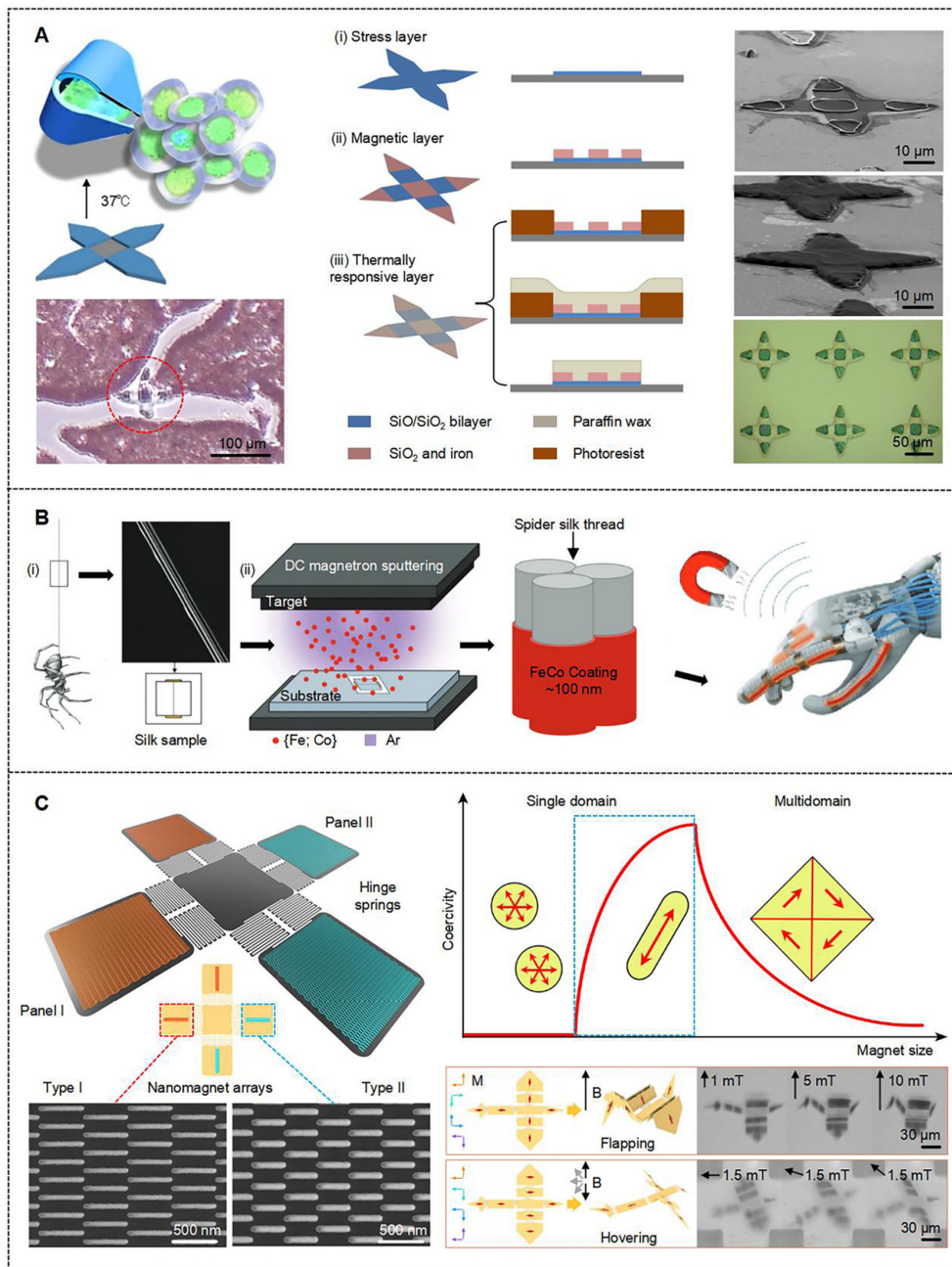


Figure 4. Soft robotics based on magnetic nanomembranes/nanostructures. (A) Untethered single cell grippers. Left and middle frames: schematics of the fabrication process for single cell grippers. (i) Deposition and pattern of the silicon monoxide (SiO) and silicon dioxide (SiO₂) as the stress layer. (ii) Deposition and pattern of silicon dioxide and iron as the rigid segments for magnetic actuation. (iii) Pattern of the paraffin layer. Right frames: SEM images of a gripper without the paraffin layer (top right), a gripper with paraffin layer (middle right), and optical image of an array of single cell grippers from (bottom right). Reproduced with permission from Ref.^[133]. Copyright © 2020. American Chemical Society; (B) Fabrication process and envisioned application of a magnetostriuctive spider silk thread. Reproduced with permission from Ref.^[142]. Copyright © 2022. John Wiley and Sons; (C) A four-panel microrobot programmed by arranging panels with nanomagnets of different sizes. Left frames: schematic illustration and SEM images of the nanomagnet arrays. Top right frame: size dependence of the coercivity of the magnets. Bottom right frames: schematics and images of a microscale ‘bird’ operated in two flying modes. Reproduced with permission from Ref.^[53]. Copyright © 2019. Springer Nature. SEM: Scanning electron microscopy.

reverse panel I due to the higher coercivity associated with the larger size. Such programming processes allow the robot to possess distinct magnetization directions at different positions, thus generating complex deformations under the trigger of the magnetic field. Additional design strategies to achieve more complicated deformations include constructing nanomagnet arrays with more than two aspect ratios and directions on multiple panels and conceiving sophisticated planar layouts that resemble recognizable objects. As an example, the bottom right frame of [Figure 4C](#) shows an origami microscale ‘bird’ consisting of nanomagnet arrays with eight different configurations. The ‘bird’ can exhibit morphological changes that resemble flapping under a magnetic field with a fixed direction and varied intensity (from 1 to 10 mT), and hovering under a rotating magnetic field with a fixed intensity of 1.5 mT.

In conclusion, magnetic nanomembranes afford remote controllability for many soft structures, thereby supporting applications in biopsy sampling, targeted drug delivery, artificial muscles, and others. Magnetic materials with other nanoscale structures, such as nanorods in cobalt, exhibit size-dependent coercivity that can be used for programmable magnetization. These advantages suggest promise for the development of soft robots with multifunctionality and multimodality.

SOFT ROBOTICS BASED ON MAGNETIC COMPOSITES

Compared with magnetic nanomembranes, magnetic composites—mixtures of magnetic particles/NWs and polymer matrices—exhibit lower modulus and, sometimes, intrinsic stretchability to enable more complex motion modalities. Unlike magnetic nanomembranes that exploit conventional lithography and deposition processes, manufacturing of magnetic composites usually adopts 3D printing, soft lithography, and laser/mechanical cutting^[132,145-149]. The overall dimensions of soft robots based on magnetic composites are usually in millimeter or centimeter scale, larger than those constructed with lithographic techniques.

One advantage of magnetic composites is that their mechanical and magnetic properties can be tailored for different applications. The polymer matrix determines the mechanical properties, while the magnetic particles/NWs play a major role in magnetic properties and motion modalities. Typically, magnetic particles can be classified into three categories: hard-magnetic (large hysteresis, high coercivity and remanence), soft-magnetic (small hysteresis, low coercivity and remanence) and superparamagnetic (no hysteresis, zero remanence)^[150], depending on the magnetic hysteresis loop.

Hard-magnetic particles retain constant magnetism once magnetized, because of their large magnetic hysteresis characterized by high coercivity and high remanence. The magnetic moments in both isotropic (e.g., NdFeB particles) and anisotropic (e.g., platelet-shaped barium hexaferrite particles) hard-magnetic particles can act as distributed and stable actuation sources to induce bending and rotation of the robots^[58]. Furthermore, the remanent magnetization within the composite matrix can be programmed in a nonuniform format through template-assisted magnetization, maskless lithography, modular assembly, and other approaches to enable complex deformations^[121,151,152]. [Figure 5A](#) demonstrates a magneto-elastic multimodal millimeter-scale robot composed of a silicone elastomer (i.e., Ecoflex 00-10) doped with hard-magnetic NdFeB particles (average diameter: 5 μm)^[153], with a single-wavelength harmonic magnetization profile along its body. The magnetization process starts with wrapping a rectangular composite on a cylinder. Applying a strong magnetic field of 1.65 T along the radial direction of the cylinder magnetizes the ring-shaped composite. Unwrapping the composite yields a flat membrane (length: 3.7 mm, width: 1.5 mm, thickness: 0.185 mm) with harmonic magnetization. Such a configuration enables different modes of locomotion when combined with spatiotemporal control of the actuating magnetic fields. For example, a periodic magnetic field is able to sequentially adapt the robot’s tilting angle and curvature, making it walk in a desired direction; while a rotating magnetic field can produce a longitudinal traveling wave to propel the robot along the direction of the wave, allowing it to crawl across obstacles.

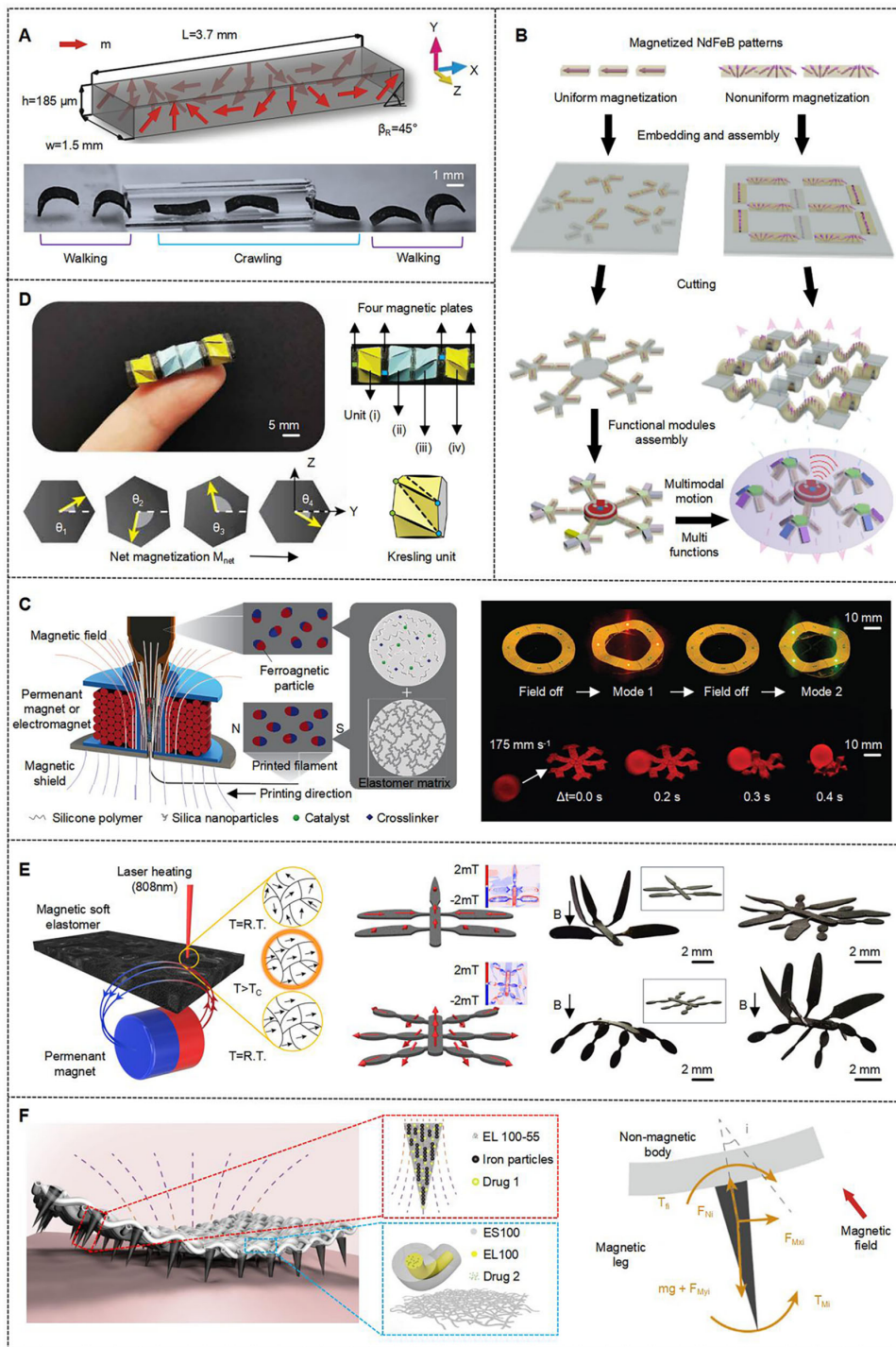


Figure 5. Soft robotics based on magnetic composites. (A) A rectangular-sheet-shaped magnetic soft robot. *m*: magnetization; *L*: length; *h*: thickness; *w*: width; β_R : phase shift in *m*. Top frame: magnetization profile. Bottom frame: photo of the robot moving a tubular tunnel (diameter 1.62 mm). Reproduced with permission from Ref. [153]. Copyright © 2018. Springer Nature; (B) The schematic diagram of integrating magnetized NdFeB patterns and functional modules for programmable and multifunctional magnetic soft robots. Reproduced with permission from Ref. [154]. Copyright © 2022. The American Association for the Advancement of Science; (C) A 3D printed magnetic soft robot. Left frame: schematics of the printing process and the material composition. Right frame: a reconfigurable soft electronic device based on the annular ring structure showing different electronic functions depending on the direction of an applied magnetic field of 30 mT (top); and a hexapedal structure stopping and holding a fast-moving object upon application of a

magnetic field generated by a permanent magnet (bottom). Reproduced with permission from Ref.^[160]. Copyright © 2018. Springer Nature; (D) An origami crawler with a four-unit Kresling origami structure and four magnetic plates. Reproduced with permission from Ref.^[161]. Copyright © 2022. The American Association for the Advancement of Science; (E) A reprogrammable magnetic soft robot. Left frame: schematic illustration of the heat-assisted 3D magnetic programming method. R.T., room temperature. Right frames: illustrations and images of various 3D shapes. Reproduced with permission from Ref.^[164]. Copyright © 2020. The American Association for the Advancement of Science; (F) A biodegradable robot based on soft-magnetic composites. Left frame: Schematic illustration of the multi-legged array and nanofiber-constructed body. Right frame: mechanical analysis of a single leg. Reproduced with permission from Ref.^[170]. Copyright © 2022. Elsevier. EL: Eudragit L; ES: Eudragit S; NdFeB: neodymium iron boron.

Another effective means to broaden the motion modalities of soft robots based on hard-magnetic composites is to prepare multiple hard-magnetic composites with uniform/nonuniform magnetizations and assemble them with controlled position and direction. [Figure 5B](#) shows a method of manufacturing untethered magnetic soft robots using modular magnetization units embedded into a network of adhesive sticker layers^[154]. Each unit contains NdFeB particles (average diameter of 38.0, 75.0, or 150.0 μm), magnetized into either uniform or nonuniform magnetization profiles by the template-assisted method. Selectively sticking the units onto a double-sided adhesive (i.e., polyetherimide (PEI) tape) forms the soft robot with complex patterns, with a planar resolution of 40 μm . After cutting out from the tape, the magnetic torque induced by the actuating magnetic field will deform the robots into various 3D geometries. In areas without magnetic particles, their shapes remain flat under a magnetic field, thereby providing the desired spaces for further integration of other functional modules, such as temperature/UV sensors and radio frequency identifiers.

The above examples mainly exploit 2D patterns with programmed magnetizations to yield multimodal locomotion. Constructing soft robots in sophisticated 3D geometries can further broaden the motion modalities^[155-159]. Soft robots based on magnetic composites are compatible with 3D printing techniques, as the composites usually undergo a precured condition that can be printed through a nozzle. [Figure 5C](#) illustrates an advanced 3D printing process that allows magnetization of the composite during the construction of the 3D structure^[160]. Here, the ink used for printing is a mixture of NdFeB particles, silica nanoparticles and an uncured elastomer matrix. Controlling the weight ratio of silica nanoparticles enables adjustment of mechanical properties (e.g., shear thinning, shear yielding) of the ink to meet the requirements for printing. Applying a magnetic field generated by a permanent magnet or an electromagnet placed around the dispensing nozzle can reorient the NdFeB particles during the printing process. Therefore, this strategy can control the position and direction of magnetization during the construction of various 3D structures. The resulting 3D soft robots exhibit many advanced geometries and motion modalities, ranging from a thin-walled structure that can elongate in its diagonal direction to a set of auxetic structures that can shrink in different directions, and to a hexapedal structure that can warp, roll, and hold objects.

Although soft robots with programmed magnetization exhibit a diverse set of motion modalities, the relatively low modulus (typically ranging from tens of kPa to dozens of MPa) of the composite materials limits the ability of the robots to overcome the large environmental resistance introduced by confined spaces. Designing origami structures to cooperate with distributed magnetic programming represents an effective approach to tackling this issue. [Figure 5D](#)^[161] shows a crawler that exploits a four-unit Kresling origami structure to generate axial contraction under either torque or compressive force^[162,163]. Rational design allows the structure to cancel out internal twists for efficient straight motion. Specifically, the structure incorporates four magnetic plates made of a mixture of silicone elastomer and hard-magnetic

particles (i.e., NdFeB), each of which locates between the two units. Adjusting the volume fraction of the magnetic particles can tune the magnetization density, thereby affecting the direction and magnitude of the torque. Such design strategies enable the programming of the torque distribution on the Kresling crawler under magnetic fields. As a result, the magnetic field can regulate the stiffness of the crawler along its axis due to the programmable torque on each Kresling unit. In the case that all the units contract simultaneously, the actuation force during crawling is sufficient to overcome the large environmental resistance. Using magnetic actuation, the crawler has the capability to steer its trajectory through rotation, suggesting promises for many medical applications such as navigation in narrow spaces inside the human body.

Many soft robots based on hard-magnetic composites leverage programmable magnetization position, direction and intensity to achieve various locomotion, but their magnetization profiles remain constant and cannot be reprogrammed to adapt to different applications. At elevated temperatures (i.e., above Curie temperature), magnetic particles can demagnetize. Therefore, simultaneously controlling the distributions of temperature and magnetic field over the hard-magnetic composites can enable reprogrammable shape transformation of magnetic soft robots^[164]. Figure 5E shows a soft robot based on a mixture of chromium dioxide (CrO_2) microparticles (average diameter: 10 μm) and a PDMS elastomer. A laser can heat a specific region of the composite to 118 $^\circ\text{C}$ (above Curie temperature) to demagnetize the magnetic particles. Applying an external magnetic field during cooling can reprogram the magnetic domains. As shown in the right frames of Figure 5E, multiple steps of laser heating and magnetization yield discrete magnetization in various 3D directions across the bodies and extremities of the robots. Such magnetization profiles allow the robot to exhibit sophisticated 3D deformations under a constant vertical magnetic field (intensity: 60 mT). The thermal-assisted strategy enables magnetic reprogramming at the microscale, with spatial resolutions up to $\sim 38 \mu\text{m}$, showing great potential in microrobots for minimally invasive medical applications. Besides laser heating, magnetothermal effect also enables reprogrammable shape conversion of soft robots^[165].

Compared with hard-magnetic particles, the coercivity and the remanence of soft-magnetic materials, such as iron and nickel- or silicon-based alloys of iron, are relatively low, leading to small magnetic hysteresis and instability under interference. However, the high magnetic susceptibility and saturation magnetization of soft-magnetic materials make them highly sensitive to magnetic fields and easy to be magnetized, thereby creating many opportunities for robotic applications^[166-169]. Figure 5F shows a biodegradable soft magnetic millirobot (Fibot) where the body exploits a core-shell structure in drug-coated nanofiber (core: Eudragit L (EL) 100 and drug2; shell: Eudragit S [ES] 100) and the legs are based on magnet-drug composites EL 100-55 containing iron particles and drug1^[170]. The soft-magnetic property of iron particles renders a positive correlation between the magnetization of the legs and the strength of the external magnetic field, and enables stable and controllable actuation of Fibot. The right frame of Figure 5F illustrates the mechanical analysis of a single leg. The angle difference θ between the easy magnetization axis of the leg i and the direction of the applied magnetic field causes a magnetic torque T_{Mi} which keeps acting on the leg until the difference disappears. Placing a permanent magnet nearby and moving it in a pre-designed trajectory allows the Fibot to achieve various locomotion^[171], such as flap-wave or inverted-pendulum motion, realizing better movement in the complex environment inside the human body. Due to the high magnetic susceptibility of soft-magnetic materials, Fibot enables the embedded iron particles to be well-arranged in an orderly manner along the leg during the fabrication. The resulting benefits include improved efficiency and quality in device manufacturing, and rapid and precise response *in vivo*, even under a small magnetic field.

Table 2. Advantages of magnetic nanomaterials in soft electronics and robotics

Advanced or unique properties	Representative examples	Functions	Improved performances
Magnetoresistance effect	GMR	Perceive the presence of static or dynamic magnetic field	Expanding the sensing capability of the human skins
	AMR	Distinguish the direction of magnetic field	Providing a better navigation ability
	TMR	High MR ratios	Enabling higher sensitivity
Size-dependent coercivity	Nanomagnets	Programmable shapes using different dimensions with various coercivity	Offering means to achieve tunable shapes and sensitivities
	Iron nanowires	Afford high remanence and coercivity to some soft magnetic materials	
Structure-dependent magnetic field	Porous matrix	Provide giant magnetoelastic effect	Enabling the devices to sense mechanical deformations
	Cilia	Measure a variety of mechanical stimuli	Improving perception in different directions
	Pyramids	Offer a magnetically permeable path to yield a more concentrated magnetic flux at the tip	Locally enhancing the magnetization
Programmable magnetization ¹	Template assisted magnetization	Allow for sophisticated deformations and locomotion	Enhancing capabilities in manipulation and deformation
	Thermally assisted magnetization		
	3D printing assisted magnetization		

AMR: Anisotropic magnetoresistance; GMR: giant magnetoresistance; MR: magnetoresistance; TMR: tunneling magnetoresistance.

The examples shown in this section prove that soft robots based on magnetic composites can adopt a diverse set of materials, including micro/nanoparticles in NdFeB, Fe, FePt, CrO₂ and other magnetic materials as the filler^[172-175], and silicone elastomers, hydrogels, and polymers as the matrix^[167,176-179], to achieve programmable deformation and multifunctional integration. Other examples in this area include programmable and reprocessible elastomer sheets for manufacturing multifunctional soft origami robots^[180], biotic-abiotic hybrid systems for *in vivo* targeted therapy^[181], and facile fabrication methods to create microrobots with functional heterogeneous materials, complex 3D geometries, as well as 3D programmable magnetization profiles^[182].

CONCLUSION AND PROSPECT

This review provides an overview of recent progress in soft electronics and robotics based on magnetic nanomaterials by classifying the materials into magnetic nanomembranes/nanostructures and magnetic composites. Table 2 summarizes the advantages of using magnetic nanomaterials in soft electronics and robotics. Soft electronics based on these magnetic nanomaterials have shown significant potential in applications of non-contact electronic skin, wearable compass, highly sensitive tactile or strain sensors, and integrated medical tools with the capability of wireless *in vivo* navigation. Meanwhile, soft robots built with magnetic nanomaterials provide vast application foreground for targeted drug delivery, precise cell manipulation, and programmable, multimodal locomotion, due to the advantages of magnetic actuation such as remote controllability, programmability, transparency to biological tissues, and compatibility with many advanced manufacturing approaches.

One of the future opportunities in this area lies in the development of advanced materials. For soft electronics, a promising yet challenging goal is to develop materials with properties (e.g., resistance) highly sensitive to the intensity and/or direction of a magnetic field. The target is to achieve sensitivities beyond existing TMR materials and replace SQUID and OPM techniques that are tethered to wires or optical fibers. An envisioned application is the acquisition of magnetocardiography (MCG), magnetoencephalography

(MEG) and other electrophysiological signals of the human body outside of hospital/laboratory settings in a wireless, continuous manner, simply by measuring the resistance change of the material. For soft robotics, the synthesis and fabrication of high-performance and biocompatible magnetic materials can open avenues for many biomedical applications. Most magnetic materials are either biologically toxic (e.g., NdFeB, Ni and Co)^[183-186] or vulnerable to biofluids (e.g., Fe and Fe₂O₃)^[187,188]. Although some magnetic materials, such as FePt, show good biocompatibility and stability^[189], their remanence and coercivity demand further improvement to compete with state-of-the-art hard-magnetic materials.

The other opportunity is to invent new manufacturing schemes for magnetic nanomaterials. On the one hand, applications in soft electronics, in many cases, rely on heterogeneous integrations of multiple functional components. The requirements on high temperature and/or large magnetic field for GMR/AMR/TMR materials, and the incompatibility with lithographic techniques for some silicone elastomers impede the integration of these materials with other functional components. Developing transfer printing schemes or other similar processes to assemble magnetic soft electronics and other sensors, stimulators, radios, circuits, etc. into the same system in a parallel and large-scale fashion represents a means to mitigate this issue. On the other hand, micro/nano manipulation and minimally invasive surgery represent promising applications of soft robotics, in which case the dimensions of the robots need to be in submillimeter or micro scale. Manufacturing approaches that can build microscale 3D robots with multi-material integration are, therefore, essential for practical applications. Some recently developed procedures, such as compressive buckling and stress-induced bending^[158,190,191], can play important roles in this area after proper adaptations.

In summary, soft electronics and robotics based on magnetic nanomaterials are of interest for applications such as human-machine interface, multimodal sensing, and biomedicine. These emerging soft magnetic systems add to a growing body of capabilities in sensing and actuation. Further developments in materials and manufacturing approaches create more opportunities in areas ranging from environmental sensing and minimally invasive surgeries to continuous, wireless monitoring and mapping of health status. These magnetic soft electronics and robotics have the potential to integrate with existing systems to broaden their functions and promote practical applications. These collective advances hold promise to revolutionize a wide range of fields, including biomedicine, electronics, and fundamental research in physics and materials science.

DECLARATIONS

Authors' contributions

Initiated the idea: Lin X, Han M

Did the literature review: Lin X

Outlined the manuscript structure: Lin X, Han M

Wrote the manuscript draft: Lin X

Designed and formatted the figures: Lin X

Reviewed and revised the manuscript: Lin X, Han M

All authors have read the manuscript and approved the final version.

Availability of data and materials

Not applicable.

Financial support and sponsorship

This work was supported by the National Natural Science Foundation of China (No. 62104009), and the Emerging Engineering Interdisciplinary Project, Peking University, the Fundamental Research Funds for the Central Universities.

Conflicts of interest

All authors declared that there are no conflicts of interest.

Ethical approval and consent to participate

Not applicable.

Consent for publication

Not applicable.

Copyright

© The Author(s) 2023.

REFERENCES

1. Zhou M, Qi Z, Xia Z, et al. Miniaturized soft centrifugal pumps with magnetic levitation for fluid handling. *Sci Adv* 2021;7:eabi7203. DOI PubMed PMC
2. Kim DC, Shim HJ, Lee W, Koo JH, Kim DH. Material-based approaches for the fabrication of stretchable electronics. *Adv Mater* 2020;32:e1902743. DOI
3. Rus D, Tolley MT. Design, fabrication and control of soft robots. *Nature* 2015;521:467-75. DOI PubMed
4. Wang C, Wang C, Huang Z, Xu S. Materials and structures toward soft electronics. *Adv Mater* 2018;30:e1801368. DOI
5. Jung D, Lim C, Shim HJ, et al. Highly conductive and elastic nanomembrane for skin electronics. *Science* 2021;373:1022-6. DOI
6. Zhao G, Ling Y, Su Y, et al. Laser-scribed conductive, photoactive transition metal oxide on soft elastomers for Janus on-skin electronics and soft actuators. *Sci Adv* 2022;8:eabp9734. DOI PubMed PMC
7. Wang B, Thukral A, Xie Z, et al. Flexible and stretchable metal oxide nanofiber networks for multimodal and monolithically integrated wearable electronics. *Nat Commun* 2020;11:2405. DOI PubMed PMC
8. Rogers JA, Someya T, Huang Y. Materials and mechanics for stretchable electronics. *Science* 2010;327:1603-7. DOI PubMed
9. Kim DH, Viventi J, Amsden JJ, et al. Dissolvable films of silk fibroin for ultrathin conformal bio-integrated electronics. *Nat Mater* 2010;9:511-7. DOI PubMed PMC
10. Song YM, Xie Y, Malyarchuk V, et al. Digital cameras with designs inspired by the arthropod eye. *Nature* 2013;497:95-9. DOI
11. Guo CF, Liu Q, Wang G, et al. Fatigue-free, superstretchable, transparent, and biocompatible metal electrodes. *Proc Natl Acad Sci U S A* 2015;112:12332-7. DOI PubMed PMC
12. Cianchetti M, Laschi C, Menciassi A, Dario P. Biomedical applications of soft robotics. *Nat Rev Mater* 2018;3:143-53. DOI
13. Maeder-york P, Clites T, Boggs E, et al. Biologically inspired soft robot for thumb rehabilitation1. *J Med Devices* 2014;8:020933. DOI
14. Kwon K, Kim JU, Deng Y, et al. An on-skin platform for wireless monitoring of flow rate, cumulative loss and temperature of sweat in real time. *Nat Electron* 2021;4:302-12. DOI
15. Wen DL, Deng HT, Liu X, Li GK, Zhang XR, Zhang XS. Wearable multi-sensing double-chain thermoelectric generator. *Microsyst Nanoeng* 2020;6:68. DOI PubMed PMC
16. Shin S, So H. Time-dependent motion of 3D-printed soft thermal actuators for switch application in electric circuits. *Additive Manufacturing* 2021;39:101893. DOI
17. Shin S, Ko B, So H. Structural effects of 3D printing resolution on the gauge factor of microcrack-based strain gauges for health care monitoring. *Microsyst Nanoeng* 2022;8:12. DOI PubMed PMC
18. Kim DH, Lu N, Ma R, et al. Epidermal electronics. *Science* 2011;333:838-43. DOI
19. Park SI, Brenner DS, Shin G, et al. Soft, stretchable, fully implantable miniaturized optoelectronic systems for wireless optogenetics. *Nat Biotechnol* 2015;33:1280-6. DOI PubMed PMC
20. Guo Y, Zhang X, Wang Y, et al. All-fiber hybrid piezoelectric-enhanced triboelectric nanogenerator for wearable gesture monitoring. *Nano Energy* 2018;48:152-60. DOI
21. Trimmer B. Soft robots. *Curr Biol* 2013;23:R639-41. DOI PubMed
22. Wang H, Totaro M, Beccai L. Toward perceptive soft robots: progress and challenges. *Adv Sci (Weinh)* 2018;5:1800541. DOI PubMed PMC
23. Breger JC, Yoon C, Xiao R, et al. Self-folding thermo-magnetically responsive soft microgrippers. *ACS Appl Mater Interfaces* 2015;7:3398-405. DOI PubMed PMC
24. Fusco S, Sakar MS, Kennedy S, et al. An integrated microrobotic platform for on-demand, targeted therapeutic interventions. *Adv Mater* 2014;26:952-7. DOI
25. Eristoff S, Kim SY, Sanchez-Botero L, Buckner T, Yirmibeşoğlu OD, Kramer-Bottiglio R. Soft actuators made of discrete grains. *Adv Mater* 2022;34:e2109617. DOI PubMed
26. Heiden A, Preninger D, Lehner L, et al. 3D printing of resilient biogels for omnidirectional and exteroceptive soft actuators. *Sci*

- Robot* 2022;7:eabk2119. DOI
27. Jang KI, Li K, Chung HU, et al. Self-assembled three dimensional network designs for soft electronics. *Nat Commun* 2017;8:15894. DOI PubMed PMC
 28. Rich SI, Wood RJ, Majidi C. Untethered soft robotics. *Nat Electron* 2018;1:102-12. DOI
 29. Zhao H, Cheng X, Wu C, et al. Mechanically guided hierarchical assembly of 3D mesostructures. *Adv Mater* 2022;34:e2109416. DOI
 30. Service RF. Technology. Electronic textiles charge ahead. *Science* 2003;301:909-11. DOI PubMed
 31. Weng W, Chen P, He S, Sun X, Peng H. Smart electronic textiles. *Angew Chem Int Ed Engl* 2016;55:6140-69. DOI
 32. Wang X, Dong L, Zhang H, Yu R, Pan C, Wang ZL. Recent progress in electronic skin. *Adv Sci (Weinh)* 2015;2:1500169. DOI PubMed PMC
 33. Liu X. The more and less of electronic-skin sensors. *Science* 2020;370:910-1. DOI PubMed
 34. Feiner R, Engel L, Fleischer S, et al. Engineered hybrid cardiac patches with multifunctional electronics for online monitoring and regulation of tissue function. *Nat Mater* 2016;15:679-85. DOI PubMed PMC
 35. Sitti M. Miniature soft robots — road to the clinic. *Nat Rev Mater* 2018;3:74-5. DOI
 36. Horvath MA, Wamala I, Rytkin E, et al. An intracardiac soft robotic device for augmentation of blood ejection from the failing right ventricle. *Ann Biomed Eng* 2017;45:2222-33. DOI PubMed PMC
 37. Han M, Chen L, Aras K, et al. Catheter-integrated soft multilayer electronic arrays for multiplexed sensing and actuation during cardiac surgery. *Nat Biomed Eng* 2020;4:997-1009. DOI PubMed PMC
 38. Kim Y, Parada GA, Liu S, Zhao X. Ferromagnetic soft continuum robots. *Sci Robot* 2019;4:eaax7329. DOI PubMed
 39. Zhao C, Ding L, Huangfu J, Zhang J, Yu G. Research progress in anisotropic magnetoresistance. *Rare Met* 2013;32:213-24. DOI
 40. Heidari H. Electronic skins with a global attraction. *Nat Electron* 2018;1:578-9. DOI
 41. Bermúdez GS, Fuchs H, Bischoff L, Fassbender J, Makarov D. Electronic-skin compasses for geomagnetic field-driven artificial magnetoreception and interactive electronics. *Nat Electron* 2018;1:589-95. DOI
 42. Fujiwara K, Oogane M, Kanno A, et al. Magnetocardiography and magnetoencephalography measurements at room temperature using tunnel magneto-resistance sensors. *Appl Phys Express* 2018;11:023001. DOI
 43. Wang M, Wang Y, Peng L, Ye C. Measurement of triaxial magnetocardiography using high sensitivity tunnel magnetoresistance sensor. *IEEE Sensors J* 2019;19:9610-5. DOI
 44. Caruso L, Wunderle T, Lewis CM, et al. In vivo magnetic recording of neuronal activity. *Neuron* 2017;95:1283-1291.e4. DOI PubMed PMC
 45. Bermúdez GS, Makarov D. Magnetosensitive e-skins for interactive devices. *Adv Funct Mater* 2021;31:2007788. DOI
 46. Ge J, Wang X, Drack M, et al. A bimodal soft electronic skin for tactile and touchless interaction in real time. *Nat Commun* 2019;10:4405. DOI PubMed PMC
 47. Melzer M, Makarov D, Calvimontes A, et al. Stretchable magnetoelectronics. *Nano Lett* 2011;11:2522-6. DOI
 48. Stuchly M, Dawson T. Interaction of low-frequency electric and magnetic fields with the human body. *Proc IEEE* 2000;88:643-64. DOI
 49. Tenforde T. Biological interactions of extremely-low-frequency electric and magnetic fields. *Chem Interf Electrochem* 1991;320:1-17. DOI
 50. Schenck JF. Physical interactions of static magnetic fields with living tissues. *Prog Biophys Mol Biol* 2005;87:185-204. DOI PubMed
 51. Zhang L, Abbott JJ, Dong L, Kratochvil BE, Bell D, Nelson BJ. Artificial bacterial flagella: Fabrication and magnetic control. *Appl Phys Lett* 2009;94:064107. DOI
 52. Luo Z, Dao TP, Hrabeč A, et al. Chirally coupled nanomagnets. *Science* 2019;363:1435-9. DOI
 53. Cui J, Huang TY, Luo Z, et al. Nanomagnetic encoding of shape-morphing micromachines. *Nature* 2019;575:164-8. DOI
 54. Li C, Lau GC, Yuan H, et al. Fast and programmable locomotion of hydrogel-metal hybrids under light and magnetic fields. *Sci Robot* 2020;5:eabb9822. DOI
 55. Wu Y, Zhang S, Yang Y, Li Z, Wei Y, Ji Y. Locally controllable magnetic soft actuators with reprogrammable contraction-derived motions. *Sci Adv* 2022;8:eabo6021. DOI PubMed PMC
 56. Cho KW, Sunwoo SH, Hong YJ, et al. Soft bioelectronics based on nanomaterials. *Chem Rev* 2022;122:5068-143. DOI
 57. Choi S, Lee H, Ghaffari R, Hyeon T, Kim DH. Recent advances in flexible and stretchable bio-electronic devices integrated with nanomaterials. *Adv Mater* 2016;28:4203-18. DOI
 58. Kim Y, Zhao X. Magnetic soft materials and robots. *Chem Rev* 2022;122:5317-64. DOI PubMed PMC
 59. Gibertini M, Koperski M, Morpurgo AF, Novoselov KS. Magnetic 2D materials and heterostructures. *Nat Nanotechnol* 2019;14:408-19. DOI
 60. Wu S, Hu W, Ze Q, Sitti M, Zhao R. Multifunctional magnetic soft composites: a review. *Multifunct Mater* 2020;3:042003. DOI PubMed PMC
 61. Murzin D, Mapps DJ, Levada K, et al. Ultrasensitive magnetic field sensors for biomedical applications. *Sensors (Basel)* 2020;20:1569. DOI PubMed PMC
 62. Lin G, Makarov D, Schmidt OG. Magnetic sensing platform technologies for biomedical applications. *Lab Chip* 2017;17:1884-912. DOI PubMed

63. Fagaly RL. Superconducting quantum interference device instruments and applications. *Rev Sci Instrum* 2006;77:101101. DOI
64. Vasyukov D, Anahory Y, Embon L, et al. A scanning superconducting quantum interference device with single electron spin sensitivity. *Nat Nanotechnol* 2013;8:639-44. DOI
65. Alexandrov EB. Recent progress in optically pumped magnetometers. *Physica Scripta* 2003;T105:27. DOI
66. Tierney TM, Holmes N, Mellor S, et al. Optically pumped magnetometers: From quantum origins to multi-channel magnetoencephalography. *Neuroimage* 2019;199:598-608. DOI PubMed PMC
67. Binasch G, Grünberg P, Saurenbach F, Zinn W. Enhanced magnetoresistance in layered magnetic structures with antiferromagnetic interlayer exchange. *Phys Rev B Condens Matter* 1989;39:4828-30. DOI PubMed
68. Baibich MN, Broto JM, Fert A, et al. Giant magnetoresistance of (001)Fe/(001)Cr magnetic superlattices. *Phys Rev Lett* 1988;61:2472-5. DOI
69. Thompson SM. The discovery, development and future of GMR: The Nobel Prize 2007. *J Phys D: Appl Phys* 2008;41:093001. DOI
70. Berkowitz AE, Mitchell JR, Carey MJ, et al. Giant magnetoresistance in heterogeneous Cu-Co alloys. *Phys Rev Lett* 1992;68:3745-8. DOI
71. Tsymbal E, Pettifor D. Perspectives of giant magnetoresistance. *Solid State Phys* :2001. pp. 113-237. DOI
72. Naoe M, Miyamoto Y, Nakagawa S. Preparation of Ni-Fe/Cu multilayers with low coercivity and GMR effect by ion beam sputtering. *J Appl Phys* 1994;75:6525-7. DOI
73. Wang L, Hu Z, Zhu Y, et al. Electric field-tunable giant magnetoresistance (GMR) sensor with enhanced linear range. *ACS Appl Mater Interfaces* 2020;12:8855-61. DOI
74. Parkin SSP, K. P. Roche KPR, Takao Suzuki TS. Giant magnetoresistance in antiferromagnetic Co/Cu multilayers grown on Kapton. *Jpn J Appl Phys* 1992;31:L1246. DOI
75. Melzer M, Lin G, Makarov D, Schmidt OG. Stretchable spin valves on elastomer membranes by predetermined periodic fracture and random wrinkling. *Adv Mater* 2012;24:6468-72. DOI PubMed
76. Makarov D, Melzer M, Karnaushenko D, Schmidt OG. Shapeable magneto-electronics. *Appl Phys Rev* 2016;3:011101. DOI
77. Melzer M, Kaltenbrunner M, Makarov D, et al. Imperceptible magneto-electronics. *Nat Commun* 2015;6:6080. DOI PubMed PMC
78. Hua Q, Sun J, Liu H, et al. Skin-inspired highly stretchable and conformable matrix networks for multifunctional sensing. *Nat Commun* 2018;9:244. DOI PubMed PMC
79. Karnaushenko D, Makarov D, Yan C, Streubel R, Schmidt OG. Printable giant magnetoresistive devices. *Adv Mater* 2012;24:4518-22. DOI PubMed
80. Ha M, Cañón Bermúdez GS, Kosub T, et al. Printable and stretchable giant magnetoresistive sensors for highly compliant and skin-conformal electronics. *Adv Mater* 2021;33:e2005521. DOI PubMed
81. Kondo M, Melzer M, Karnaushenko D, et al. Imperceptible magnetic sensor matrix system integrated with organic driver and amplifier circuits. *Sci Adv* 2020;6:eaay6094. DOI PubMed PMC
82. Cañón Bermúdez GS, Makarov D. Geometrically curved magnetic field sensors for interactive electronics. In: Makarov D, Sheka DD, editors. *Curvilinear micromagnetism*. Cham: Springer International Publishing; 2022. pp. 375-401. DOI
83. Becker C, Karnaushenko D, Kang T, et al. Self-assembly of highly sensitive 3D magnetic field vector angular encoders. *Sci Adv* 2019;5:eaay7459. DOI PubMed PMC
84. Melzer M, Karnaushenko D, Lin G, Baunack S, Makarov D, Schmidt OG. Direct transfer of magnetic sensor devices to elastomeric supports for stretchable electronics. *Adv Mater* 2015;27:1333-8. DOI PubMed PMC
85. Swastika P, Antarnusa G, Suharyadi E, Kato T, Iwata S. Biomolecule detection using wheatstone bridge giant magnetoresistance (GMR) sensors based on CoFeB spin-valve thin film. *J Phys : Conf Ser* 2018;1011:012060. DOI
86. Cañón Bermúdez GS, Karnaushenko DD, Karnaushenko D, et al. Magnetosensitive e-skins with directional perception for augmented reality. *Sci Adv* 2018;4:eaao2623. DOI PubMed PMC
87. Becker C, Bao B, Karnaushenko DD, et al. A new dimension for magnetosensitive e-skins: active matrix integrated micro-origami sensor arrays. *Nat Commun* 2022;13:2121. DOI PubMed PMC
88. Maury P, Monteil B, Marty L, Duparc A, Mondoly P, Rollin A. Three-dimensional mapping in the electrophysiological laboratory. *Arch Cardiovasc Dis* 2018;111:456-64. DOI PubMed
89. Rivkin B, Becker C, Singh B, et al. Electronically integrated microcatheters based on self-assembling polymer films. *Sci Adv* 2021;7:eabl5408. DOI PubMed PMC
90. Wang Z, Wang X, Li M, et al. Highly Sensitive flexible magnetic sensor based on anisotropic magnetoresistance effect. *Adv Mater* 2016;28:9370-7. DOI
91. Oliveros Mata ES, Cañón Bermúdez GS, Ha M, et al. Printable anisotropic magnetoresistance sensors for highly compliant electronics. *Appl Phys A* 2021:127. DOI
92. Guo Y, Deng Y, Wang SX. Multilayer anisotropic magnetoresistive angle sensor. *Sens Actuator A Phys* 2017;263:159-65. DOI
93. Rittinger J, Taptimthong P, Jogschies L, Wurz MC, Rissing L. Impact of different polyimide-based substrates on the soft magnetic properties of NiFe thin films. *Proc Spie* 2015:9517. DOI
94. Quynh LK, Tu BD, Anh CV, et al. Design optimization of an anisotropic magnetoresistance sensor for detection of magnetic nanoparticles. *Journal of Elec Materi* 2019;48:997-1004. DOI
95. Chiolerio A, Allia P, Celasco E, Martino P, Spizzo F, Celegato F. Magnetoresistance anisotropy in a hexagonal lattice of Co antidots obtained by thermal evaporation. *J Mag Magn Mater* 2010;322:1409-12. DOI

96. Rijks TG, Coehoorn R, de Jong MJ, de Jonge WJ. Semiclassical calculations of the anisotropic magnetoresistance of NiFe-based thin films, wires, and multilayers. *Phys Rev B Condens Matter* 1995;51:283-91. DOI PubMed
97. Popovic RS, Drljaca PM, Schott C In Bridging the gap between AMR, GMR, and Hall magnetic sensors, 2002 23rd International Conference on Microelectronics. Proceedings (Cat. No.02TH8595), 12-15 May 2002; 2002; pp 55-58 vol.1. DOI
98. Michelena MD, Oelschlägel W, Arruego I, del Real RP, Mateos JAD, Merayo JM. Magnetic giant magnetoresistance commercial off the shelf for space applications. *J Appl Phys* 2008;103:07E912. DOI
99. Grissom CB. Magnetic Field Effects in Biology: A Survey of Possible Mechanisms with Emphasis on Radical-Pair Recombination. *Chem Rev* 1995;95:3-24. DOI
100. Djayaprawira DD, Tsunekawa K, Nagai M, et al. 230% room-temperature magnetoresistance in CoFeB/MgO/CoFeB magnetic tunnel junctions. *Appl Phys Lett* 2005;86:092502. DOI
101. Ikeda S, Hayakawa J, Ashizawa Y, et al. Tunnel magnetoresistance of 604% at 300K by suppression of Ta diffusion in CoFeB/MgO/CoFeB pseudo-spin-valves annealed at high temperature. *Appl Phys Lett* 2008;93:082508. DOI
102. Carlson A, Bowen AM, Huang Y, Nuzzo RG, Rogers JA. Transfer printing techniques for materials assembly and micro/nanodevice fabrication. *Adv Mater* 2012;24:5284-318. DOI PubMed
103. Chung H, Kim T, Kim H, et al. Fabrication of releasable single-crystal silicon-metal oxide field-effect devices and their deterministic assembly on foreign substrates. *Adv Funct Mater* 2011;21:3029-36. DOI
104. Loong LM, Lee W, Qiu X, et al. Flexible mgo barrier magnetic tunnel junctions. *Adv Mater* 2016;28:4983-90. DOI
105. Ota S, Ono M, Matsumoto H, et al. CoFeB/MgO-based magnetic tunnel junction directly formed on a flexible substrate. *Appl Phys Express* 2019;12:053001. DOI
106. Ota S, Ando A, Sekitani T, Koyama T, Chiba D. Flexible CoFeB/MgO-based magnetic tunnel junctions annealed at high temperature (≥ 350 °C). *Appl Phys Lett* 2019;115:202401. DOI
107. Saito K, Imai A, Ota S, Koyama T, Ando A, Chiba D. CoFeB/MgO-based magnetic tunnel junctions for film-type strain gauge. *Appl Phys Lett* 2022;120:072407. DOI
108. Ribeiro P, Cardoso S, Bernardino A, Jamone L. Highly sensitive bio-inspired sensor for fine surface exploration and characterization. *Ieee Int Conf Robot* :2020. 625-631. DOI
109. Ye C, Wang Y, Tao Y. High-density large-scale tmr sensor array for magnetic field imaging. *IEEE Trans Instrum Meas* 2019;68:2594-601. DOI
110. Amaral J, Pinto V, Costa T, et al. Integration of TMR sensors in silicon microneedles for magnetic measurements of neurons. *IEEE Trans Magn* 2013;49:3512-5. DOI
111. Wang SX, Bae S, Li G, et al. Towards a magnetic microarray for sensitive diagnostics. *J Magn Magn Mater* 2005;293:731-6. DOI
112. Li D, Yao K, Gao Z, Liu Y, Yu X. Recent progress of skin-integrated electronics for intelligent sensing. *Light: Advanced Manufacturing* 2021;2:4. DOI
113. Chen JY, Lau YC, Coey JM, Li M, Wang JP. High performance MgO-barrier magnetic tunnel junctions for flexible and wearable spintronic applications. *Sci Rep* 2017;7:42001. DOI PubMed PMC
114. Chow TS. The effect of particle shape on the mechanical properties of filled polymers. *J Mater Sci* 1980;15:1873-88. DOI
115. Varga Z, Filipcsei G, Zrínyi M. Magnetic field sensitive functional elastomers with tuneable elastic modulus. *Polymer* 2006;47:227-33. DOI
116. Diguët G, Sebald G, Nakano M, Lallart M, Cavaillé J. Magnetic particle chains embedded in elastic polymer matrix under pure transverse shear and energy conversion. *J Magn Magn Mater* 2019;481:39-49. DOI
117. Diguët G, Sebald G, Nakano M, Lallart M, Cavaillé J. Optimization of magneto-rheological elastomers for energy harvesting applications. *Smart Mater Struct* 2020;29:075017. DOI
118. Zhou Y, Zhao X, Xu J, et al. Giant magnetoelastic effect in soft systems for bioelectronics. *Nat Mater* 2021;20:1670-6. DOI
119. Zhao X, Chen G, Zhou Y, et al. Giant magnetoelastic effect enabled stretchable sensor for self-powered biomonitoring. *ACS Nano* 2022;16:6013-22. DOI
120. Li Y, Qi Z, Yang J, et al. Origami NdFeB flexible magnetic membranes with enhanced magnetism and programmable sequences of polarities. *Adv Funct Mater* 2019;29:1904977. DOI
121. Zhao Y, Gao S, Zhang X, et al. Fully flexible electromagnetic vibration sensors with annular field confinement origami magnetic membranes. *Adv Funct Mater* 2020;30:2001553. DOI
122. Yan Y, Hu Z, Yang Z, et al. Soft magnetic skin for super-resolution tactile sensing with force self-decoupling. *Sci Robot* 2021;6:eabc8801. DOI
123. Hellebrekers T, Kroemer O, Majidi C. Soft Magnetic skin for continuous deformation sensing. *Adv Intell Syst* 2019;1:1900025. DOI
124. Wang H, de Boer G, Kow J, et al. Design methodology for magnetic field-based soft tri-axis tactile sensors. *Sensors (Basel)* 2016;16:1356. DOI PubMed PMC
125. Tomo TP, Regoli M, Schmitz A, et al. A new silicone structure for uskin—a soft, distributed, digital 3-axis skin sensor and its integration on the humanoid robot icub. *IEEE Robot Autom Lett* 2018;3:2584-91. DOI
126. Theilade UA, Hansen HN. Surface microstructure replication in injection molding. *Int J Adv Manuf Technol* 2007;33:157-66. DOI
127. Isaacoff BP, Brown KA. Progress in top-down control of bottom-up assembly. *Nano Lett* 2017;17:6508-10. DOI PubMed
128. Alfadhel A, Kosel J. Magnetic nanocomposite cilia tactile sensor. *Adv Mater* 2015;27:7888-92. DOI PubMed
129. Zhang X, Zheng C, Li Y, Wu Z, Huang X. Magnetically levitated flexible vibration sensors with surficial micropylam arrays for

- magnetism enhancement. *ACS Appl Mater Interfaces* 2022;14:37916-25. DOI
130. Câmara Santa Clara Gomes T, Abreu Araujo F, Piraux L. Making flexible spin caloritronic devices with interconnected nanowire networks. *Sci Adv* 2019;5:eav2782. DOI PubMed PMC
131. Bharti B, Fameau AL, Rubinstein M, Velev OD. Nanocapillarity-mediated magnetic assembly of nanoparticles into ultraflexible filaments and reconfigurable networks. *Nat Mater* 2015;14:1104-9. DOI PubMed PMC
132. Fan X, Rong Y, Xu J, Liu W, Chen L, Huang Y. Study on HAZ of nanosecond UV laser cutting multilayer ferrite ceramic composite flakes for electromagnetic shielding. *J Mater Sci: Mater Electron* 2022;33:24354-66. DOI
133. Jin Q, Yang Y, Jackson JA, Yoon C, Gracias DH. Untethered single cell grippers for active biopsy. *Nano Lett* 2020;20:5383-90. DOI PubMed PMC
134. Reddy AN, Maheshwari N, Sahu DK, Ananthasuresh GK. Miniature compliant grippers with vision-based force sensing. *IEEE Trans Robot* 2010;26:867-77. DOI
135. Gultepe E, Randhawa JS, Kadam S, et al. Biopsy with thermally-responsive untethered microtools. *Adv Mater* 2013;25:514-9. DOI PubMed PMC
136. Cecchi R, Verotti M, Capata R, et al. Development of micro-grippers for tissue and cell manipulation with direct morphological comparison. *Micromachines* 2015;6:1710-28. DOI
137. Liu W, Jia X, Wang F, Jia Z. An in-pipe wireless swimming microrobot driven by giant magnetostrictive thin film. *Sens Actuator A Phys* 2010;160:101-8. DOI
138. Chen XZ, Hoop M, Shamsudhin N, et al. Hybrid magnetoelectric nanowires for nanorobotic applications: fabrication, magnetoelectric coupling, and magnetically assisted in vitro targeted drug delivery. *Adv Mater* 2017;29:1605458. DOI
139. Hristoforou E, Ktena A. Magnetostriction and magnetostrictive materials for sensing applications. *J Magn Magn Mater* 2007;316:372-8. DOI
140. Olabi A, Grunwald A. Design and application of magnetostrictive materials. *Materials & Design* 2008;29:469-83. DOI
141. Atulashimha J, Flatau AB. A review of magnetostrictive iron-gallium alloys. *Smart Mater Struct* 2011;20:043001. DOI
142. Spizzo F, Greco G, Del Bianco L, Coisson M, Pugno NM. Magnetostrictive and Electroconductive Stress-Sensitive Functional Spider Silk. *Adv Funct Materials* 2022;32:2207382. DOI
143. Chakraverty S, Bandyopadhyay M. Coercivity of magnetic nanoparticles: a stochastic model. *J Phys : Condens Matter* 2007;19:216201. DOI
144. Skomski R, Zhou J, Nanomagnetic Models. In *Advanced Magnetic Nanostructures*, Sellmyer D, Skomski R, Eds. Springer US: Boston, MA, 2006. pp 41-90. DOI
145. Pishvar M, Amirkhosravi M, Altan MC. Magnet assisted composite manufacturing: A novel fabrication technique for high-quality composite laminates. *Polym Compos* 2019;40:159-69. DOI
146. Wei X, Jin M, Yang H, Wang X, Long Y, Chen Z. Advances in 3D printing of magnetic materials: Fabrication, properties, and their applications. *J Adv Ceram* 2022;11:665-701. DOI
147. Błyskun P, Kowalczyk M, Łukaszewicz G, Grabias A, Zackiewicz P, Kolano-burian A. Low-porosity soft magnetic mouldable composites. *Materialia* 2022;26:101602. DOI
148. Ślusarek B, Przybylski M. Hard and soft magnetic composites with modified magnetic properties. *World J. Eng* 2011;8:87-92. DOI
149. Zhang J, Guo Y, Hu W, Soon RH, Davidson ZS, Sitti M. Liquid crystal elastomer-based magnetic composite films for reconfigurable shape-morphing soft miniature machines. *Adv Mater* 2021;33:e2006191. DOI PubMed PMC
150. Coey J. Magnetic materials. *J. Alloys Compd* 2001;326:2-6. DOI
151. Kim J, Chung SE, Choi SE, Lee H, Kim J, Kwon S. Programming magnetic anisotropy in polymeric microactuators. *Nat Mater* 2011;10:747-52. DOI PubMed
152. Lum GZ, Ye Z, Dong X, et al. Shape-programmable magnetic soft matter. *Proc Natl Acad Sci U S A* 2016;113:E6007-15. DOI PubMed PMC
153. Hu W, Lum GZ, Mastrangeli M, Sitti M. Small-scale soft-bodied robot with multimodal locomotion. *Nature* 2018;554:81-5. DOI PubMed
154. Dong Y, Wang L, Xia N, et al. Untethered small-scale magnetic soft robot with programmable magnetization and integrated multifunctional modules. *Sci Adv* 2022;8:eabn8932. DOI PubMed PMC
155. Cheng Y, Chan KH, Wang XQ, et al. Direct-ink-write 3D printing of hydrogels into biomimetic soft robots. *ACS Nano* 2019;13:13176-84. DOI
156. Xue Z, Jin T, Xu S, et al. Assembly of complex 3D structures and electronics on curved surfaces. *Sci Adv* 2022;8:eabm6922. DOI PubMed PMC
157. Cheng X, Zhang Y. Micro/Nanoscale 3D assembly by rolling, folding, curving, and buckling approaches. *Adv Mater* 2019;31:e1901895. DOI PubMed
158. Miao L, Song Y, Ren Z, et al. 3D temporary-magnetized soft robotic structures for enhanced energy harvesting. *Adv Mater* 2021;33:e2102691. DOI PubMed
159. Yang Q, Liu T, Xue Y, et al. Ecoresorbable and bioresorbable microelectromechanical systems. *Nat Electron* 2022;5:526-38. DOI
160. Kim Y, Yuk H, Zhao R, Chester SA, Zhao X. Printing ferromagnetic domains for untethered fast-transforming soft materials. *Nature* 2018;558:274-9. DOI PubMed
161. Ze Q, Wu S, Nishikawa J, et al. Soft robotic origami crawler. *Sci Adv* 2022;8:eabm7834. DOI PubMed PMC

162. Li Z, Kidambi N, Wang L, Wang K. Uncovering rotational multifunctionalities of coupled Kresling modular structures. *Extreme Mech Lett* 2020;39:100795. DOI
163. Kaufmann J, Bhovad P, Li S. Harnessing the multistability of kresling origami for reconfigurable articulation in soft robotic arms. *Soft Robot* 2022;9:212-23. DOI PubMed
164. Alapan Y, Karacakol AC, Guzelhan SN, Isik I, Sitti M. Reprogrammable shape morphing of magnetic soft machines. *Sci Adv* 2020;6. DOI PubMed PMC
165. Tang J, Sun B. Reprogrammable shape transformation of magnetic soft robots enabled by magnetothermal effect. *Appl Phys Lett* 2022;120:244101. DOI
166. Tang Z, Xu Z, Bo X, et al. Magnetically controlled flexible micro-robots based on magnetic particle arrangement. *Mater Adv* 2023;4:1314-25. DOI
167. Schmauch MM, Mishra SR, Evans BA, Velev OD, Tracy JB. Chained iron microparticles for directionally controlled actuation of soft robots. *ACS Appl Mater Interfaces* 2017;9:11895-901. DOI PubMed
168. Bayaniahangar R, Bayani Ahangar S, Zhang Z, Lee BP, Pearce JM. 3-D printed soft magnetic helical coil actuators of iron oxide embedded polydimethylsiloxane. *Sens Actuators B Chem* 2021;326:128781. DOI
169. Maria-Hormigos R, Mayorga-Martinez CC, Pumera M. Soft magnetic microrobots for photoactive pollutant removal. *Small Methods* 2023;7:e2201014. DOI PubMed
170. Tan R, Yang X, Lu H, et al. Nanofiber-based biodegradable millirobot with controllable anchoring and adaptive stepwise release functions. *Matter* 2022;5:1277-95. DOI
171. Lu H, Zhang M, Yang Y, et al. A bioinspired multilegged soft millirobot that functions in both dry and wet conditions. *Nat Commun* 2018;9:3944. DOI PubMed PMC
172. Li M, Ostrovsky-snider NA, Sitti M, Omenetto FG. Cutting the cord: progress in untethered soft robotics and actuators. *MRS Advances* 2019;4:2787-804. DOI
173. Sitti M, Wiersma DS. Pros and cons: magnetic versus optical microrobots. *Adv Mater* 2020;32:e1906766. DOI PubMed
174. Li L, Xin C, Hu Y, et al. On-demand maneuver of millirobots with reprogrammable motility by a hard-magnetic coating. *ACS Appl Mater Interfaces* 2022;14:52370-8. DOI
175. Zhao R, Dai H, Yao H, Shi Y, Zhou G. Shape programmable magnetic pixel soft robot. *Heliyon* 2022;8:e11415. DOI PubMed PMC
176. Li H, Go G, Ko SY, Park J, Park S. Magnetic actuated pH-responsive hydrogel-based soft micro-robot for targeted drug delivery. *Smart Mater Struct* 2016;25:027001. DOI
177. Goudu SR, Yasa IC, Hu X, Ceylan H, Hu W, Sitti M. Biodegradable untethered magnetic hydrogel milli-grippers. *Adv Funct Mater* 2020;30:2004975. DOI
178. Ze Q, Kuang X, Wu S, et al. Magnetic shape memory polymers with integrated multifunctional shape manipulation. *Adv Mater* 2020;32:e1906657. DOI PubMed
179. Zhao Y, Hua M, Yan Y, Wu S, Alsaïd Y, He X. Stimuli-responsive polymers for soft robotics. *Annu Rev Control Robot Auton Syst* 2022;5:515-45. DOI
180. Zhang S, Ke X, Jiang Q, Ding H, Wu Z. Programmable and reprocessable multifunctional elastomeric sheets for soft origami robots. *Sci Robot* 2021;6:eabd6107. DOI
181. Magdanz V, Khalil ISM, Simmchen J, et al. IRONSperm: Sperm-templated soft magnetic microrobots. *Sci Adv* 2020;6:eaba5855. DOI PubMed PMC
182. Liu Z, Li M, Dong X, Ren Z, Hu W, Sitti M. Creating three-dimensional magnetic functional microdevices via molding-integrated direct laser writing. *Nat Commun* 2022;13:2016. DOI PubMed PMC
183. Ermolli M, Menné C, Pozzi G, Serra MA, Clerici LA. Nickel, cobalt and chromium-induced cytotoxicity and intracellular accumulation in human haecac keratinocytes. *Toxicology* 2001;159:23-31. DOI PubMed
184. Lü X, Bao X, Huang Y, Qu Y, Lu H, Lu Z. Mechanisms of cytotoxicity of nickel ions based on gene expression profiles. *Biomaterials* 2009;30:141-8. DOI PubMed
185. Ahamed M. Toxic response of nickel nanoparticles in human lung epithelial A549 cells. *Toxicol In Vitro* 2011;25:930-6. DOI PubMed
186. Magaye R, Zhao J, Bowman L, Ding M. Genotoxicity and carcinogenicity of cobalt-, nickel- and copper-based nanoparticles. *Exp Ther Med* 2012;4:551-61. DOI PubMed PMC
187. Cabot A, Puentes VF, Shevchenko E, et al. Vacancy coalescence during oxidation of iron nanoparticles. *J Am Chem Soc* 2007;129:10358-60. DOI
188. Sun YP, Li XQ, Cao J, Zhang WX, Wang HP. Characterization of zero-valent iron nanoparticles. *Adv Colloid Interface Sci* 2006;120:47-56. DOI PubMed
189. Kadiri VM, Bussi C, Holle AW, et al. Biocompatible Magnetic Micro- and Nanodevices: Fabrication of FePt Nanopropellers and Cell Transfection. *Adv Mater* 2020;32:e2001114. DOI PubMed
190. Rafsanjani A, Bertoldi K, Studart AR. Programming soft robots with flexible mechanical metamaterials. *Sci Robot* 2019;4:eaav7874. DOI PubMed
191. Han M, Guo X, Chen X, et al. Submillimeter-scale multimaterial terrestrial robots. *Sci Robot* 2022;7:eabn0602. DOI